Atmos. Meas. Tech. Discuss., https://doi.org/10.5194/amt-2017-336
Manuscript under review for journal Atmos. Meas. Tech.
Discussion started: 12 October 2017

Atmospheric Measurement Techniques Discussions

Increased aerosols content in the atmosphere over Ukraine during summer 2010

Evgenia Galytska[1], Vassyl Danylevsky[2], René Hommel[1,*], and John P. Burrows[1]

[1]Institute of Environmental Physics, University of Bremen, Bremen, Germany
[2]Taras Schevchenko National University, Kyiv, Ukraine
[*]now at Hommel & Graf Environmental, Hamburg, Gottingen, Germany

Correspondence to: Evgenia Galytska (egalytska@iup.physik.uni-bremen.de)

Abstract. In this paper we assess the influence of one of the most important sources of aerosols in the atmosphere, biomass burning, during summer 2010 on the abundance, dynamics, and properties of aerosols over Ukraine, also considering influences and effects over neighboring countries: ETR, Estonia, Belarus, Poland, Moldova, and Romania.

MODIS satellite instrument data were used to study fires distribution. Ground-based remote measurements from the international sun photometers network AERONET and MODIS and CALIOP satellite instruments data were used to determine aerosols content and optical properties in the atmosphere over East Europe. HYSPLIT model was used to further investigate atmospheric dynamics and to simulate pathways of particles transport.

We found that the highest air pollution was observed over Moscow in the first half of August 2010, apparently due to the proximity of the most active combustion centers. Significant temporal dynamics of the aerosols content with pronounced pollution peaks during August 7–17 was observed at Ukrainian (Kyiv, Sevastopol), Belarusian (Minsk), Estonian (Toravere) and Romanian (Bucharest) AERONET sites.

Aerosols spatio-temporal distribution over Ukraine were constructed and analyzed using MODIS AOD 550 nm data validated by Kyiv AERONET site sunphotometer measurements, and CALIOP AOD 532 nm validated by MODIS AOD data. Vertical distribution of aerosols extinction at 532 nm, retrieved from the measurements by CALIOP, were constructed for the territory of Ukraine at locations where high AOD values were observed during intense wildfires. The influence of the fires on the optical and microphysical properties of aerosol particles, such as size distribution, spectral single-scattering albedo and refractive indices, was analyzed and estimated using Kyiv AERONET measurements, performed during summer 2010.

In this study we show that the highest aerosols pollution over Ukraine recorded on summer 2010 was caused by particles transported from the forest fires in Russia. These fires caused the highest AOD 440 nm over Kyiv site, which for August 2010 exceeded the mean value for the same month for the entire observational period by factor of two. Also, the influence of fires resulted in a change of particles microphysical properties in the regions, where pollution was the highest.

1 Introduction

Biomass burning is well known to be a significant global source of trace gases and aerosols in the atmosphere (Seiler and Crutzen, 1980; Crutzen and Andreae, 1990). For example, Barnaba et al. (2011) stated that wildfires (mixture of peat burning

Atmos. Meas. Tech. Discuss., https://doi.org/10.5194/amt-2017-336
Manuscript under review for journal Atmos. Meas. Tech.
Discussion started: 12 October 2017

Atmospheric Measurement Techniques Discussions

and forest fires) significantly contribute to the fine mode (particles size < 1 μm) aerosols optical depth (AOD). The largest numbers of these fires occur in Africa, Asia and South America, but a not negligible fraction also occurs in Eastern Europe and former USSR countries, particularly in the Russian Federation, Ukraine and Kazakhstan. In recent years, considerable attention by the international scientific community was paid to the impact on pollution of the aerosols from fires in central and western regions of Russia in summer 2010. Increased interest in these events is the result of the occurrence of the fires and significant air pollution in populated areas of Russia, and combustion products comprising gases and aerosols that are spread over large areas of Eastern Europe. Over the past few years, a significant amount of research has been done on the spatial and temporal distribution of aerosols in summer 2010 over Eastern Europe. The papers provided results on aerosol distribution and properties and their impact on air quality in the atmosphere over the area occupied by fires and neighboring territories, are Konovalov et al. (2011); Witte et al. (2011); Péré et al. (2014); Chubarova et al. (2012).

Chubarova et al. (2012) analyzed aerosols properties and radiative effects during 2010 fire events in Central Russia according to ground-based measurements AERONET in Moscow and Zvenigorod, as well as radiative measurements with a WMO calibrated pyranometers located in Moscow. An extremely high AOD was observed in Moscow and its suburbs on August 6-8, with an absolute maximum at 500 nm on August 7 reaching 6.4 at Moscow and 5.9 at Zvenigorod. Spatial distribution of AOD has been retrieved for these dates using MODIS satellite data. Chubarova et al. (2012) analyzed how smoke affects the key aerosols properties, such as particle size distribution, refractive index (RI), SSA, and the phase function asymmetry factor. These quantities, measured during fire events, were compared 1) with those obtained earlier in-between the fires in same regions and 2) with analogous aerosol properties determined during wildfires but at other regions of the globe. They also assessed the impact of wildfire products on the incoming solar irradiance in different ranges of the optical spectrum, including UV-range, and estimated the radiative forcing (RF) at the top of the atmosphere (TOA). Chubarova et al. (2012) also explored the impact of intense fires on the environment. Significant change in the atmospheric gas composition, aerosols concentration, and air temperature caused detrimental influence on human health. Particularly the mortality rate increased by 1.5–1.6 times in the central region of ETR during summer 2010 (Chubarova et al., 2012). Konovalov et al. (2011) analyzed the evolution of near-surface concentrations of carbon-monoxide (CO), PM_{10} and ozone (O_3) in Moscow region during the summer 2010 heat wave by comparing available ground-based and satellite measurements with mesoscale model simulations. They used a modified version of the CHIMERE chemistry transport model (http://www.lmd.polytechnique.fr/chimere/) to include wildfire emissions of primary pollutants and the shielding effect of smoke aerosols on photolysis. They used measurements, which were collected at automated monitoring stations with a nominal measurement frequency of three measurements per hour (in Zvenigorod, Zelenograd, and Pavlovskii Posad). Fire radiative power (FRP) data retrieved from the measurements performed by Moderate-Resolution Imaging Spectrometer (MODIS) on board of National Aeronautics and Space Administration (NASA) Aqua and Terra satellites were used to study spatial and temporal variability of fire activities. AOD measured by MODIS at 550 nm was also used to correct a negative bias in FRP measurements in case of fires obscured by heavy smoke.

Konovalov et al. (2011) also analyzed SSA retrieved from AErosol RObotic NETwork (AERONET) measurements performed in Moscow during the period of major fire events in summer 2002. It was found that the extreme air pollution episodes in Moscow were mainly caused by fires taking place at relatively short distance (less than 200 km) from the measurement site;

Atmos. Meas. Tech. Discuss., https://doi.org/10.5194/amt-2017-336
Manuscript under review for journal Atmos. Meas. Tech.
Discussion started: 12 October 2017

Atmospheric Measurement Techniques Discussions

the transport of air pollution from more distant fires was found rather in-significant. They also showed that a compensation of a possible negative bias in the measured FRP obscured by heavy smoke is a crucial procedure for a good performance of the model.

These events influenced the content and characteristics of aerosols in the atmosphere not only above burning areas but also over most of Eastern Europe, where the fires were not as strong as in ETR and eastern Ukraine. The tropospheric dynamics of aerosols pollution over these territories has been studied by Witte et al. (2011) by means of ground-based and satellite observations. They applied data from satellite instruments MODIS and OMI (Ozone Monitoring Instrument) in the area between 45–63°N and 23–63°E (including territory over Ukraine). They studied the spatial and temporal distribution and energy characteristics of burning cells using MODIS AOD at 550 nm, and OMI aerosol index (AI) at 354 nm, AOD, and SSA (both at 388 nm). Their results correlate well with the development of synoptic situation determined by back-trajectory simulations with the starting point in Moscow. Meteorological parameters, such as vertical temperature profiles, pressure, humidity, and wind direction were determined according to radiosonde measurements over the ETR.

The aerosol shortwave direct RF during the peak of 2010 Russian wildfires and their feedbacks on air temperature and atmospheric dynamics was described by Péré et al. (2014), who used CHIMERE offline coupled to the meso-scale WRF (Weather Research and Forecasting) community model. This paper analyzes the impact of fine aerosol particles (10 nm–5 μm) on shortwave (0.2–6.0 mm) solar radiation. Aerosol direct RF and feedbacks in the atmosphere were simulated for the period August 5–12, 2010 on the basis of observational data obtained with ground-based AERONET sunphotometers, and POLDER (POLarization and Directionality of the Earth's Reflectances) and CALIOP (Cloud-Aerosol Lidar with Orthogonal Polarization) satellite instruments. AOD, SSA and asymmetry factor of aerosol particles were analyzed. Vertical distribution of aerosols was determined from the vertical profiles of CALIOP extinction coefficient measurements at 532 nm wavelength. Strong perturbations of atmospheric composition over Russia were clearly detectable from these various data. Moscow was subjected to an important aerosol radiative effect, especially during the arrival of the aerosol plume on August 6–10.

The above-mentioned studies are focused in Moscow and other Russian areas. Satellite data and modeling studies hardly cover adjacent territories, including Ukraine. Only a few studies explored aerosol properties and aerosol impacts over Ukraine during severe wildfire events. Witte et al. (2011) provided AI, SSA, AOD 550 nm data averaged over the period of active fires (from July 22 to August 2010), including the domain of latitudes 45–52°N and longitudes 23–33°E, where Ukraine is located. These data show significantly lower aerosol pollution of the atmosphere over Ukraine in comparison with western and central regions of ETR, although MODIS observed fire cells in the eastern part of Ukraine during the same period. According to Péré et al. (2014), AOD 550 nm measured by POLDER and modeled for particular days of August 5–12, the assessments of RF and air pollution impact on the near-surface air temperature over Ukraine are much lower than over central regions of ETR. However, in other previously published studies by means of POLDER satellite and AERONET ground-based measurements (Bovchaliuk et al., 2013; Milinevsky et al., 2014) was reported a marked increase of aerosol content in the atmosphere over Kyiv and some regions of Ukraine during summer 2010 in comparison with other years.

In this paper, we present results of in-detail studies of tropospheric aerosol pollution over Ukraine during summer 2010. We use available data of ground-based AERONET sunphotometer measurements, satellite data from MODIS Aqua and Terra and

Atmos. Meas. Tech. Discuss., https://doi.org/10.5194/amt-2017-336
Manuscript under review for journal Atmos. Meas. Tech.
Discussion started: 12 October 2017

Atmospheric Measurement Techniques Discussions

CALIOP instruments. The meteorological situation was reproduced from air mass back trajectory simulations with HYSPLIT model. We estimate spatio-temporal influence of extensive biomass burning in Eastern Europe on air pollution caused by aerosols over Ukraine and neighboring areas, which was not the focus of above mentioned studies. We also evaluate available data of aerosols properties and content in the atmosphere, measured by the ground-based (AERONET) and satellite (MODIS, CALIOP) instruments.

2 Data sources

2.1 AERONET data

Among all available methods of remote sensing of aerosols properties in the atmosphere, the most reliable data is derived from ground-based measurements of direct solar irradiation and sky radiation by automatic sunphotometers AERONET. This network was founded by NASA and the PHOtométrie pour le Traitement Opérationnel de Normalisation Satellitaire (PHOTONS); Lille1 University, National Centre for Space Studies CNES, and the National Center for Scientific Research of France CNRS and includes several hundreds of AERONET sites over the world. The basic principle of the network is to standardize and metrology the equipment, the technique of measurement and processing of data, which are stored in a freely accessible centralized database. Description of instruments and measurements procedures, data processing, calibration of sunphotometers, the accuracy of measurements and terminology are described in Holben et al. (1998) and in the documentation from AERONET web page (http://aeronet.gsfc.nasa.gov/). According to AERONET classification, all observed data are divided into 3 levels: Level 1.0 – primary unscreened data, Level 1.5 – cloud-screened data, Level 2.0 – highest accuracy data, cloud-screened and quality-controlled and corrected for sunphotometers recalibration. We used Level 2.0 data in our research. Spectral AOD in the atmospheric column over the observational site is determined from direct solar irradiance measurements with errors of ± 0.01 in the visible and near-infrared regions of the spectrum and with a larger uncertainty (± 0.02) in the UV band Holben et al. (1998). The Angstrom exponent (AE) is defined in the range of 440-870 nm, according to the AERONET algorithm. In case of successful measurements of the sky radiance along almucantar and altitude circle of the Sun the properties of aerosol particles such as size distribution, SSA, RI, and phase function are retrieved by inverse solution (Dubovik et al., 2000; Dubovik and King, 2000).

There were only two AERONET sites in Ukraine in 2010: Kyiv (50°N, 30°E) and Sevastopol (44°N, 33°E). In this paper, we used data mostly from Kyiv site, because of predominant continental aerosol over most of Ukraine and Russia, while over Sevastopol the essential component of aerosols is sea salt as it is located in the coastal zone of Crimea. To assess the extent of the impact of forest fires in summer 2010 we also used data of neighboring Eastern European AERONET sites located in the countries. Measurements of aerosol properties over Kyiv by AERONET started at the end of March 2008 (Danylevsky et al., 2011a, b). The Kyiv PHOTONS/AERONET site is located at The Main Astronomical Observatory of the National Academy of Sciences of Ukraine at Golosiiv forest situated at the south of Kyiv, at a distance of 10 km from the city center. From 2008 until 2013, the site was equipped with the sun photometer CIMEL CE-318-2 polarized model with the filters of 440, 670, 870, 936, and 1020 nm. The surrounding landscape around Kyiv site enables the sun photometer to scan celestial hemisphere completely.

Data are sent to AERONET database twice a day and are accessed and displayed on the Kyiv AERONET web-site at the same day. Data observed during summer 2010 are of Level 2.0 quality (cloud-screened and quality-controlled data).

2.2 MODIS data

Two nearly identical MODIS instruments are installed onboard the Terra (EOS AM-1) and Aqua (EOS PM-1) satellites. Terra (http://terra.nasa.gov/about/) flies in a sun-synchronous, near-polar, circular orbit with an inclination of 98.5°at an altitude of 705 km every 98 minutes (16 orbits per day). The local equatorial crossing time is approximately 10:30 a.m. in a descending node. The Aqua satellite belongs to the afternoon A-Train constellation (http://atrain.gsfc.nasa.gov). The local equatorial crossing time is approximately 1:30 p.m. in an ascending node of a sun-synchronous, near-polar, circular orbit. MODIS data are widely used for researching the Earth's atmosphere, surface, and biosphere. To retrieve aerosol properties over land measurements at the spectral channels 0.47, 0.66, and 2.12 μm are used. From these data the following parameters are calculated with the application of appropriate algorithms: AOD at spectral channels at 0.47, 0.55, and 0.66 μm wavelength, the relative amount of fine mode aerosol particles AOD at 550 nm, and the Angstrom component in the spectral range of 0.47–0.66 μm (Remer et al., 2005; Levy et al., 2007, 2013).

We used MODIS/Aqua and MODIS/Terra Level 2 Collection 051 Optical_Depth_Land_And_Ocean product retrieved by the C005 aerosol over-land algorithm, averaged over 10 km × 10 km cells in nadir and approximately 12 km × 12 km at the edge of the field of view. Due to the wide field of view, which equals to ±55°(approximately 2300 km on the surface) cross track, MODIS can obtain observational data daily on each point of the surface in the mid-latitudes during favorable weather conditions.

We applied MODIS AOD data with 2 main purposes: 1) to compare with ground-based AERONET measurements over Kyiv site, and 2) to estimate atmospheric pollution over Ukraine caused by aerosols from wildfires. Although documentation of the MODIS Level 2 Collection 051 Optical_Depth_Land_And_Ocean Scientific Data Set (SDS; Levy et al., 2010) does not recommend application of these data for quantitative analysis, we applied them because the alternatively recommended SDS Corrected_Optical_Depth_Land contains only a very small amount of data in the regions at time period we consider in our study. Earlier studies applying the Optical_Depth_Land_And_Ocean product already showed good agreement between AOD of MODIS (Quality Assurance Confidence flags 1, 2, 3; QAC) and AERONET on global scale (Levy et al., 2010; Remer et al., 2008; Bréon et al., 2011). Therefore we apply here all data over land with QAC 1, 2, 3 from this SDS without any additional filter. We also following Levy et al. (2010) and all AOD ranged from -0.05 to 0.05 consider equal to 0.

The MODIS mission also provides fire mapping on the land surface, which we used to evaluate the activity of fires and their spatial distribution, similar to Witte et al. (2011). For detecting fires and defining their characteristics, two spectral channels (4 and 11 μm) are used by MODIS data processing algorithm (Justice et al., 2002). Combustion temperature (in K) is defined from the measurements of the spectral brightness of the flame with the application of the Stefan-Boltzmann law. A special algorithm is applied to calculate the number of burning cells and the total area occupied by fires. Data of spatio-temporal distribution of fires are freely available on the Internet (http://rapidfire.sci.gsfc.nasa.gov/cgi-bin/imagery/firemaps.cgi?period=2010221-2010230) with the support of NASA. To visualize the distribution of fires we used Fire Information for Resource

Management System (FIRMS). With this tool, active fires are detected in each pixel with a size of approximately 1 km. For more information on algorithms on fire recognition and evaluation of their intensity, the principles of archiving and distributing data can be found in Schroeder et al. (2008); Davies et al. (2009); Justice et al. (2011). In most cases, MODIS detects vegetation fires but sometimes also volcanic eruptions or flares of gas as well. Here we interpret the results of observations under conditions of forest fires and other vegetation or peat.

2.3 CALIOP data

CALIOP flies onboard the NASA Cloud–Aerosol Lidar and Infrared Pathfinder Satellite Observations (CALIPSO) satellite, which belongs to the afternoon A-Train constellation. CALIOP is a two wavelength (532 and 1064 nm) polarization lidar and provides high-resolution vertical profiles of aerosols and clouds. A detailed description is provided on its official website (http://www-calipso.larc.nasa.gov/about/) and in Winker et al. (2003); Hunt et al. (2009). CALIOP uses three receiver channels: one measures the 1064 nm backscatter intensity and two channels measure orthogonally polarized components of the 532 nm backscattered signal. The laser beam is directed almost in nadir, with a slight tilt forward in the direction of motion of the satellite to avoid direct reflection of laser radiation from high reflectivity objects (surface water, snow, etc.). The divergence of the transmitted laser beam equals 100 μrad and results in the footprint at the Earth's surface of about 70 meters. A pulse repetition rate of approximately 20 Hz provides vertical resolution of 15 m. The application of special algorithms to the CALIOP measurements of the vertical profile of the atmosphere backscatter coefficient enables to derive aerosol particles and clouds and to define vertical profiles of aerosol extinction for two wavelengths (532 and 1064 nm). Corresponding AOD is determined by extinction coefficient integration over altitude (Vaughan et al., 2009; Winker et al., 2009; Young et al., 2013; Omar et al., 2009). Vertical distribution of the extinction coefficient and AOD at 532 nm defined along the path of the sub-satellite point were used for this study. We used Level 2 Cloud and Aerosol Layer and Profile products V 3.01 and 3.02 with a resolution of 5 km on the surface along the sub-satellite point, see (CALIPSO Quality Statements Lidar Level 2 Cloud and Aerosol Layer Products, Version Releases: 3.01,3.02 https://eosweb.larc.nasa.gov/PRODOCS/calipso/Quality_Summaries/CALIOP_L2LayerProducts_3.01.html; CALIPSO Quality Statements: Lidar Level 2 Cloud and Aerosol Profile Products Version Releases: 3.01,3.02 https://eosweb.larc.nasa.gov/sites/default/files/project/calipso/quality_summaries/CALIOP_L2ProfileProducts_3.01.pdf).

2.4 Meteorological data and the means of study of air masses transport in the investigated region

To analyze the impact of weather conditions on the distribution of aerosols in the atmosphere during June-August 2010 we used synoptic maps from Ukrainian Weather Service on isobaric surfaces representing altitudes of 2 m, 1.5, 3 and 5 km. Synoptic maps of international research centers were also used, namely maps of 500 hPa/surface pressure maps from the Global Forecast System (GFS, http://www.wetterzentrale.de/topkarten) and the German Weather Service (http://www1.wetter3.de). To confirm the analysis of synoptic charts we also calculated trajectories of air masses using the Hybrid Single Particle Lagrangian Integrated Trajectory Model (HYSPLIT-4), developed by the National Oceanic and Atmospheric Administration's (NOAA) Air Resources Laboratory (ARL; Draxler and Hess, 1998; Bowman et al., 2013). HYSPLIT is freely available software (http://ready.arl.noaa.gov/HYSPLIT.php). According to Stohl (2002), the uncertainty of calculated trajectories is ±20%

Atmos. Meas. Tech. Discuss., https://doi.org/10.5194/amt-2017-336
Manuscript under review for journal Atmos. Meas. Tech.
Discussion started: 12 October 2017

in the horizontal direction for the time period more than 24 hours in the free troposphere, and after 120 hours the uncertainty increases to about 400 km in the horizontal and about 1300 m in vertical planes.

3 Methodology and results

We assess the influence of biomass burning during summer 2010 on aerosols over Ukraine and neighboring territories according to ground-based and satellite measurements and analyze the synoptic-scale situation by modeling air mass trajectories. To estimate the impact of biomass burning, we analyze data from several AERONET sites located in Eastern Europe. From all available Ukrainian AERONET stations, continental aerosols properties were measured only in Kyiv in 2010. To analyze aerosols properties over other regions of Ukraine we used MODIS data for assessing column AOD and CALIOP data for assessing column AOD and vertical distributions of aerosol extinction.

To prove our results, we also validate satellite data by comparing with ground-based AERONET measurements. The best option is when all instruments would measure optical properties of the same air mass at the same time. Since the track of CALIOP laser beam runs across the field of view of MODIS/Aqua, both devices are scanning the same air mass. However, because of differences in the fields of view of satellite instruments, in particular the small field of view of CALIOP, not many collocations are found for our comparison. Because of the Earth's rotation the trajectory of the sub-satellite point on the Earth's surface shifts to the west approximately by 24.5°(e.g. about 1880 km for the latitude 50°) during CALIPSO orbit period. Since the satellite track runs every 16 days (233 satellite rotations) along the same route the probability of the CALIOP to pass over the atmosphere column observed by the solar photometer AERONET is very low (the column radius on the earth's surface is about 10–15 km depending on the effective height of the aerosol layer and the season). Significantly higher chance of AERONET site to be into the MODIS field of view and it provides opportunities for both instruments data comparison. In the following, first we directly compare MODIS AOD to sunphotometer AOD, followed by comparing the AOD of CALIOP to MODIS.

To identify the impact of fires on air pollution by aerosols over Ukraine, including Kyiv, we analyzed the transport of air masses entering the Kyiv region in summer 2010 by calculating back trajectories of air masses during 7 days at different altitudes. To identify aerosols sources and contributions from dynamics in the atmosphere, we analyzed aerosols profiles at observational sites along the air mass trajectories. Freely available CALIOP observations are the only source of such information for areas under consideration. Since only a few profiles match collocation criteria, we examined vertical aerosols profiles and associated characteristics for the whole summer in 2010.

3.1 Impact of forest fires and weather conditions during summer 2010 on aerosols air pollution in Eastern Europe

To analyze the impact of forest fires on air pollution caused by aerosols in Fig. 1 we plotted fire distributions and total radiation intensities over Eastern Europe and the ETR in summer 2010 as observed by MODIS. Each of map contains 10-days sum of the number of burning cells from July 1 to August 20. The corresponding time-series of the total number of burning cells in the studied area (40–65°N and 10–60°E) is shown in Fig. 2. From Fig. 1 its obvious that the burning of forests, grass and

Atmos. Meas. Tech. Discuss., https://doi.org/10.5194/amt-2017-336
Manuscript under review for journal Atmos. Meas. Tech.
Discussion started: 12 October 2017

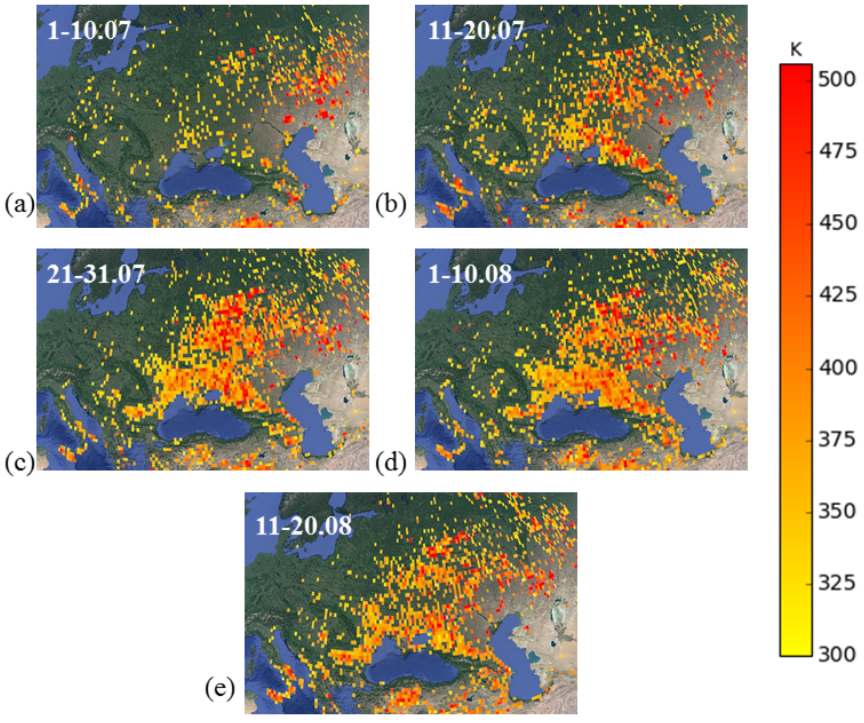

Figure 1. Localization and intensity (in K) of fires in Eastern Europe and ETR during summer 2010 according to MODIS data represented as a sum of burning cells and FRP every 10 days from July 1 to August 20: (a) July 1–10, (b) July 11–20, (c) July 21–31, (d) August 1–10, (e) August 11–20.

peat from mid-July on occurred throughout Europe, but the highest fire concentrations were observed in the ETR, Ukraine and Moldova. Both the overall number and intensity of fires in this regions reached a maximum between July 26 and August 18. The highest count of fires and also largest FRP were observed in July 29 (Fig. 1c, d and Fig. 2). Such large fire areas, intensities and durations were caused by peculiar weather conditions over ETR and Eastern Europe during the second half of summer 2010, which led to accumulation of aerosols in the atmosphere over these regions (Witte et al., 2011; Chubarova et al., 2012; Péré et al., 2014).

Ground-based AERONET observations showed an increased aerosols content over Eastern Europe sites during July and August 2010. We analyzed changes in AOD at 500 nm using all measurements on daily average, Level 2.0, from the AERONET database for the sites Minsk (Belarus), Moscow (Russian Federation), Toravere (Estonia), Belsk (Poland), Chisinau (Moldova), Cluj-Napoca, Bucharest, and Eforie (all Romania), Kyiv and Sevastopol (both Ukraine). AOD 500 nm data for the Kyiv site was obtained by data interpolation using Angstrom formula in the range of 440–870 nm. The analysis revealed a significant temporal dynamics of the aerosols content with pronounced peaks during August 15–17 in Kyiv, Sevastopol, Minsk and Bucharest (see. Table 1). This indicates the accumulation of aerosols from one source of pollution within a single synoptic process. Also, highest AOD were observed in Romania (Cluj-Napoca and Eforie sites) on August 1, in Moscow and Toravere on August 7, in

Atmos. Meas. Tech. Discuss., https://doi.org/10.5194/amt-2017-336
Manuscript under review for journal Atmos. Meas. Tech.
Discussion started: 12 October 2017

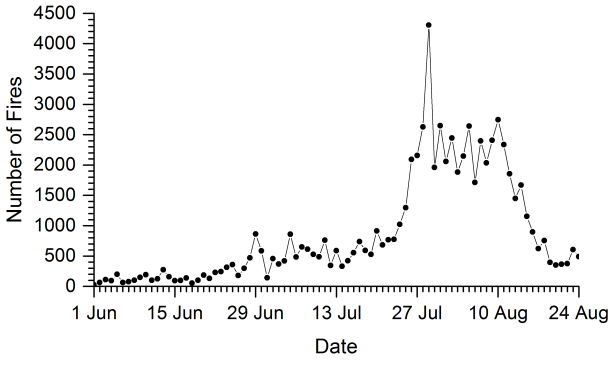

Figure 2. Average number of burning cells during summer 2010 according to MODIS Aqua and Terra data over territory of 40–65°N, 10-60°E.

Table 1. Level of air pollution caused by aerosols (AOD 500 nm) in summer 2010 over Eastern Europe according to AERONET.

Site	Number of meas.	Mean AOD	Std.Dev	Min AOD	Max AOD	Date of Max AOD
Belsk	1938	0.18	0.11	0.05	0.74	16-07-10
Bucharest	2381	0.30	0.16	0.06	0.97	17-08-10
Cluj-Napoca	1220	0.25	0.13	0.04	0.62	01-08-10
Eforie	1855	0.24	0.10	0.06	0.59	01-08-10
Kyiv	2732	0.30	0.20	0.05	1.26	15-08-10
Minsk	1368	0.25	0.20	0.04	1.27	17-08-10
Moldova	1343	0.22	0.11	0.05	0.62	13-07-10
Moscow	1573	0.36	0.46	0.05	4.62	07-08-10
Sevastopol	3564	0.23	0.12	0.04	0.93	16-08-10
Toravere	1296	0.20	0.19	0.03	1.23	07-08-10

Moldova and Belsk in July (observations from Moldova from July 25 until October are not available). The highest air pollution caused by aerosols over all analyzed territories was observed over Moscow in the first half of August, apparently due to the proximity of the most active combustion centers.

To study in-detail the aerosols inflow to the measurement sites, as given in Table 1, we computed back trajectories of air masses for each of the corresponding dates at different heights (Fig. 3). Trajectories were simulated for 168 hours (7 days) from the respective sites at altitudes of 500 m, 1.5, 3, 4, and 5 km at 12:00 GMT starting time. Back trajectories for locations where high aerosols loads were observed first, i.e. Moldova and Belsk (July 13 and 16, respectively), are shown in Fig. 3a,b. Trajectories indicate, aerosol were transported to Moldova from Europe (at the altitude of 3–4 km), from the ETR (500 m) and the Black Sea (1.5 km) throughout Ukraine. Into the region of Belsk, aerosols were transported throughout continental Europe (1,5–5 km), mostly from the Atlantic Ocean but also from the Baltic, across regions of quite active fires by that time (Fig. 1) in the lower atmosphere (500 m). Transport to two Romanian sites (Cluj-Napoca and Eforie), with maximum AOD observed on

August 1 (Fig. 3c,d), occurred in the lower layer of the atmosphere in an altitude of 1,5 km, originating from the southeast of Ukraine and Moldova (also area with active fires); at 3–4 km altitude – from the Atlantic through Europe, the Mediterranean and the Balkans; and in the highest layers (5–6 km) to Eforie from the Middle East through the Mediterranean and the Balkans.

Back trajectories for Moscow (Fig. 3e) and Toravere (Fig. 3f), with maximum AOD on August 7, correspond to anticyclonic circulation: according to back-trajectories, aerosols to Moscow were transported mostly from the surrounding regions with the most active fires. Air masses entering Toravere originated from Asian regions and crossed areas of active fires in southeastern Ukraine in all analyzed altitudes. For Kyiv (Ukraine), the AOD maximum was observed on August 15: in the lower 4-km atmospheric layer, the air movement corresponded to anticyclonic circulation, which caused the air stagnation and contaminants accumulation over the ETR and Eastern Europe; at the altitude of 5 km air was transported across the Europe from the Atlantics (Fig. 3g). On August 16, the maximum was recorded in Sevastopol on Black Sea coast, where air masses travelled in almost the entire range of heights (500 m–5 km) from the ETR and Kazakhstan through the territory of active fires in the south-west of Russia (Fig. 3h).

In Minsk and Bucharest the maximum was observed a day later on August 17 (Table 1, Fig. 3i,j). Towards Minsk, aerosols were transported from different regions at different altitudes. At 5 km, air masses came from the Mediterranean Sea through the Balkans, Romania and the western part of Ukraine; at 4 km they originate from the Alps and travelled throughout Central Europe and Poland; at 3 km from Kazakhstan across the Caspian Sea, south of Russia, and Ukraine, where the active fires were observed; at 1,5 km - from Ukraine, and at 500 m - from the western regions of the ETR through Ukraine. To Bucharest air at 500 m was transported from the north-east, specifically through the ETR and the south-east of Ukraine. At altitudes of 1.5 km and 5 km, air of Atlantic origin moved throughout Europe and entered Bucharest region. The air trajectory at 4 km is similar to the previous ones just the air originates from Iberian Peninsula, and at 3 km the air originates from Africa.

On August 18-21, a change in synoptic processes was observed: atmospheric fronts of an active cyclone, which moved from the south of Baltic region to Samara, led to a significant change of weather pattern in Eastern Europe. This change caused a distinct decrease in fires activities, wet deposition of aerosols, thus their lower content in the atmosphere above all investigated regions in the second half of August.

3.2 Aerosols dynamics over Kyiv according to AERONET measurements and analysis of back trajectories

Milinevsky et al. (2014) analyzed aerosols pollution over Ukraine for the years 2008-2013 from AERONET sunphotometer observations, also noting a significant higher AOD over Kyiv in July–August 2010. Table 2 shows our analysis of the AERONET measured aerosols content over Kyiv and its variability during the period of observation, also including 2014 for comparing with Milinevsky et al. (2014). The highest mean and median values for the year were observed in 2010 mainly due to impact of wildfires in July and August. The highest content of aerosols over Kyiv was observed every year in spring (April–May) and late summer (July–August). The lowest AOD was observed in June and in the middle of autumn, in agreement with Milinevsky et al. (2014). However, the least variable AOD during the warm period of the year was observed in June, while in June 2010 it was also one of the largest for this month. The most significant air pollution caused by aerosols for the entire period of

Atmos. Meas. Tech. Discuss., https://doi.org/10.5194/amt-2017-336
Manuscript under review for journal Atmos. Meas. Tech.
Discussion started: 12 October 2017

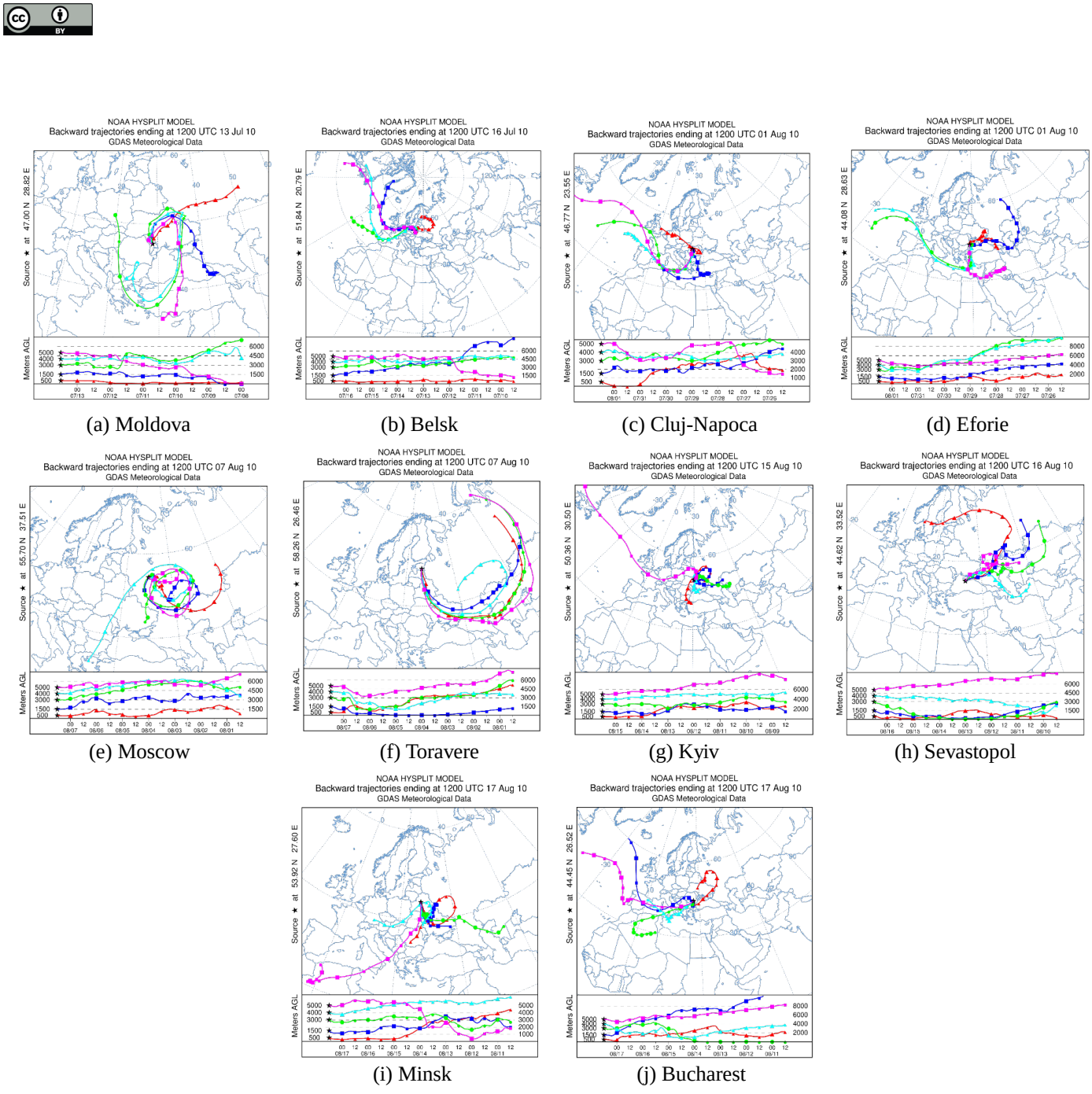

Figure 3. Back trajectories of air masses to AERONET sites on the dates with the highest AOD.

AERONET observations in Kyiv was recorded in August 2010. This event related to the active fires of vegetation in the ETR and in other parts of Eastern Europe.

Atmos. Meas. Tech. Discuss., https://doi.org/10.5194/amt-2017-336
Manuscript under review for journal Atmos. Meas. Tech.
Discussion started: 12 October 2017

Atmospheric Measurement Techniques Discussions

Table 2. Annual changes of monthly averaged AOD at 440 nm over Kyiv during the warm season for the available observational period.

AOD 440 nm							
Year	April	May	June	July	August	September	October
2008	0.181	0.253	0.239	0.178	0.338	0.310	0.222
2009	0.384	0.255	0.236	0.239	0.225	0.278	0.191
2010	0.322	0.200	0.240	0.322	0.520	0.144	0.135
2011	0.386	0.239	0.232	0.328	0.253	0.325	0.309
2012	0.275	0.241	0.212	0.205	0.248	0.150	0.157
2013	0.268	0.192	0.242	0.252	0.206	0.163	0.214
2014	0.253	0.239	0.152	0.214	0.270	0.197	0.187
Mean	0.296	0.231	0.222	0.248	0.294	0.224	0.202
					0.257(without 2010)		

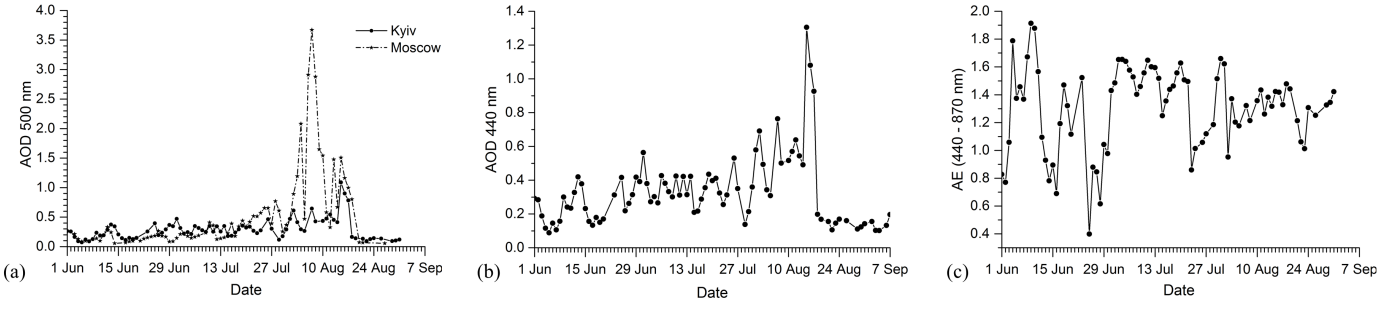

Figure 4. AOD 500 nm over Moscow and Kyiv (a), AOD 440 nm over Kyiv (b), AE over Kyiv (c).

The impact of fires on the AOD over Kyiv during summer 2010 was less distincts as over Moscow (Fig. 4). However, relative to multi-annual average conditions, also the aerosol pollution over Kyiv was exceptional. The average AOD 440 nm for August 2010 exceeds the mean value for the same month for the entire observation period (excluding 2010) by about factor two (see Table 2). In addition, the mean 500 nm AOD for June 2010 over Kyiv was approximately 0.20, while its daily average on August 15 was approximately 1.09. That is 5.5 times higher than the average AOD 500 nm for the August of the same year was 0.44. During the summer period, from early June until approximately August 18, the aerosols content over Kyiv gradually increased by more than an order of magnitude (Fig. 4a).

Computing the back trajectories of air parcels that were transported to Kyiv at altitudes of 500 m, 1.5, 3, 4 and 5 km, we analyzed the possible sources of aerosols from various regions during this period (see Supplementary material, Fig. S01–S30). AOD changes in June were defined by both local sources and the transport with air masses mainly from the western areas.

Atmos. Meas. Tech. Discuss., https://doi.org/10.5194/amt-2017-336
Manuscript under review for journal Atmos. Meas. Tech.
Discussion started: 12 October 2017

Atmospheric Measurement Techniques Discussions

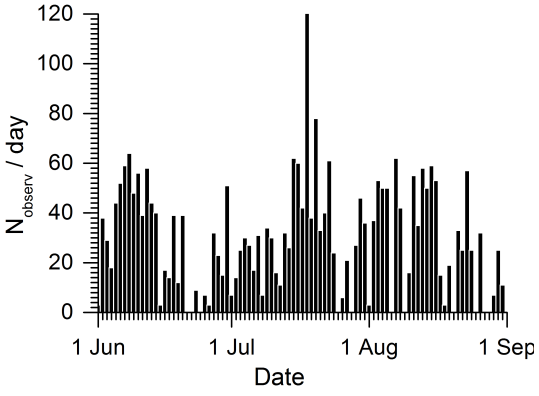

Figure 5. Number of AOD 440 nm observations per day at Kyiv AERONET site during summer 2010.

According to synoptic analysis, at the beginning of June the air in the lower 5-km of the atmosphere was transported to Ukraine from the south, mainly from North Africa and the Mediterranean Sea through the Balkans and the Black Sea. Therefore, the relative maximum AOD during June 1–2 (Fig. S01-S02) was caused by local sources and, in addition, by particles transported from southern regions, as mixtures of continental soil dust and urban-industrial aerosols with sea salt and possibly dust from Sahara. This is testified by both relatively low values of AE (Fig. 4c), and prevailing coarse mode AOD over fine mode defined by spectral deconvolution algorithm (SDA) (O'Neill et al., 2003). However, it should be noted that during these days AOD measurements were performed in partly cloudy conditions and an observational selection was considered. Thus, for June 1 we had only 3 measurements in the evening, but for June 2 there were more data (Fig. 5).

Increased AOD values during June 8–14 also were observed in the conditions of unstable weather, sometimes with clouds, however the series enable to assess the behavior of AOD for every day. Air masses in the altitudes 500 m–5 km were transported to Kyiv from the Atlantic across Scandinavia, the Baltic Sea, circulating over the Western, Central and Eastern Europe (Fig. S03-S09). The increase of AOD was caused by aerosols of different types: according to AE and SDA, on June 8–11 fine mode of aerosols prevailed, and further increase of AOD during June 12–13 was caused by the arrival of coarse mode aerosols, which explains the rapid decrease of AE (Fig. 4c). Coarse aerosol particles were mainly of local origin, while the fine mode particles likely were brought by air currents from Europe.

During June 23–26 AOD was measured in cloudy conditions, so the fact of its increase (Fig. 4a,b) cannot be considered as reliable because of the small amount of data (9 measurements in the evening of June 23, 7 measurements on June 25 and 3 measurements on June 26, Fig. 5). Herewith, the dynamics of airflow during these days was more diverse (Fig. S10-S12). At 500 m air was transported to Kyiv mainly from Kazakhstan through the steppe zone of ETR and eastern and south-eastern regions of Ukraine; at the altitudes of 1.5–5 km mainly from Turkey and the Caucasus through the Black and Azov seas, often changing direction and heights. In general, the accuracy of derived AOD values, obtained from a rather small number of individual measurements through short-term gaps in the clouds, can not be considered as sufficient. Because the algorithm of detection and elimination of the influence of clouds on measured AOD is not able to distinguish a thin uniform layer consisting

of cloud water droplets from aerosols in the sunphotometer field of view (Smirnov et al., 2000). Therefore, we do not interpret relatively high AOD values for June 27–29 as a significant aerosols load over Kyiv during these days. On June 30 the average AOD at 500 nm was equal approximately 0.35. It was computed for almost continuous dataset observed that day. This means that the aerosols content on June 30 increased comparing to the June 16–20.

During June 27–29 the dynamics of tropospheric circulation and the transport of air masses through Kyiv significantly changed (Fig. S13–S15). Preceding this period, since the beginning of June, air masses predominantly travelled to Kyiv mainly from the Atlantic throughout the European continent. However, during June 27–29 the air mass transport path changed as seen in our back trajectory calculations that moved first southward and finally eastward. So that finally from June 29 on, air in above-mentioned altitudes was transported to Kyiv from Kazakhstan and Central Asia, across the Caspian Sea, the steppe zone of the ETR, and eastern regions of Ukraine. In addition, the 500 m back trajectory indicated a rapid change of the air motion from the north-west. On 30 June air motion remained unchanged (Fig. S16).

According to our analysis of air mass transport and spatio–temporal distribution of the intensities of fires in Eastern Europe, it was seen that vegetation fires were not the main source of increased concentrations of aerosols over Kyiv in June. The complex impact of continental particles and aerosols of marine origin was dominating. The relatively high AOD value on July 1 (see Fig. 5) was observed based on less than 10 measurements during that day. There were also no more measurements the day after, on July 2. During both days, wind directions at different altitudes varied much. Air entered Kyiv on July 1 at lower altitudes (500 m–1.5 km) passing central regions of the ETR on June 28–30. At 3–5 km altitude air came from the steppe area between the Caspian Sea and the eastern border of Ukraine. As seen from Fig. 1a, a large number of fires burned there during those days. Thus, combustion products in the form of aerosols likely influenced the atmosphere over Kyiv and increased the AOD.

In the morning of July 2 air masses entered Kyiv from the North Atlantic at altitudes of 500 m–3 km; at the end of day also at altitude of 5 km (Fig. S17). In the following three days, July 3–5, when washout by rain cleaned the atmosphere in the evening of July 2nd, AERONET-measured AODs were temporarily low, with values below 0.3 at 440 nm. On these days cloudiness decreased significantly and more measurements could be taken into account, thus, decreasing the uncertainty of the derived time-series. Between July 3–5 air masses entered Kyiv from the North Atlantic and Arctic through various parts of Europe, particularly at lower altitudes (500 m–1.5 km) through the ETR (Fig. S18-S20). During July 6–7 the synoptic situation changed (Fig. S21-S22). Air masses now travelled westward at altitudes 0.5–4 km, originating mainly from central Kazakhstan and the ETR. Those air masses crossed the steppe zone of ETR and south-east Ukraine, where active fires were observed (Fig. 1a,b) and caused the relatively high AODs over Kyiv (Fig. 4a). Another rapid change in the synoptic situation and transport pathways occurred again on July 8–9: air masses came from the Atlantic coast of Western Europe, travelled eastward causing an AOD decrease over Kyiv (Fig.4b, S23-S24).

The aerosols load over Kyiv during July 10–27 (Fig.4a,b) was changing under the influence of air masses mainly coming from the Atlantic and the Arctic Ocean through the ETR, where different types of fires burned (Fig. S25). These air masses crossed Kazakhstan and steppe zones of the ETR and through south-eastern Ukraine. Air masses were also circulating over the Central and Western regions of the ETR, Belarus and Ukraine and other neighboring countries, where at that time vegetation

and peat fire were observed (Fig. S26). The number of fires and their intensity were gradually increasing towards end of July (Fig. 1b,c). Consequently, the increase of AOD over Kyiv during those days was caused by the accumulation of aerosol particles from the regions of active fires or formed under the influence of combustion products. Intermediate AOD decreases are caused by below cloud scavenging from occasional rains over Kyiv.

Rainy weather on July 27–28 over Kyiv site and a change in the transport pathways caused a significant decrease in AOD during July 29–30. Air masses entered Kyiv in the altitude range 500 m–5 km, coming from North Atlantic, passing Western Europe, the Mediterranean, the Balkans, Romania, Moldova, and western regions of Ukraine (Fig. S27).

During July 31–August 1 an increase of AOD over Kyiv was observed (Fig. 4a,b), with air masses originating over the Atlantic and traveling throughout Scandinavia, Western and Southern Europe, the Mediterranean, the Balkans, later circulating over Ukraine, the Baltics, Poland, Romania and Moldova. Likely the increase of AOD was observed due to intense biomass burning in Ukraine and neighbouring territories, as shown by Fig. 1c,d. On August 2, air masses in the altitude range 500 m–3 km were transported to Kyiv from western and central regions of the ETR, from Kazakhstan throughout North Caucasus and the steppe zone of the ETR, as well as throughout south-eastern Ukraine (Fig. S28). In those regions intense forest, peat and vegetation fires were detected at that time (Fig. 1). Accordingly, these events were the reason of aerosols pollution over this region and Ukraine in particular till August 18.

Between August 2–18 AOD over Kyiv were increasing and reached maximum values on 15 August with about 1.5 at 440 nm and 1.26 at 500 nm, respectively. This is more than factor 2 larger than during the fire period before August 2. For the following 2 days, August 16–17, the AOD level remained high. It increased so much because air masses circulated over the entire region, from Ural and Kazakhstan to Central Europe and the Baltic (Fig. S29-S30). During August 18–21 atmospheric fronts of an active cyclone, which moved from the south of the Baltics to Samara region, caused significant weather change with rains in Eastern Europe. Aerosol washout cleaned the atmosphere over investigated sites and caused the sharp AOD decrease seen in the time-series of Fig.4a,b. Until the end of analysing period, i.e. end of August 2010, the average AOD level over Kyiv remained as low as during less polluted days in June 2010.

According to SDA analysis by O'Neill et al. (2003), fine mode aerosols dominated the AOD increase over Kyiv in the periods 6–7 and 10–27 July, as well as on 31 July 2010. The 500 nm AOD reached values up to 0.1, except on July 26–27. On those two days just a few measurements (Fig. 5) were available due to cloudiness. Thus, derived AOD values are more uncertain. A similar situation was observed later in August, when relatively high AODs were found, but only due to fine mode aerosols. On August 2 and 12, the coarse mode had significant impact on the observed AOD increase and the decrease of AE (Fig. 4c).

Kyiv AERONET observations can also be used to analyze the impact of vegetation fires products on microphysical properties of aerosol particles in summer 2010. Key aerosol properties, indicating microphysical processes in an aerosols population, were retrieved by inverse solution from AERONET sun photometer measurements along the almucantar of the Sun (Dubovik et al., 2000; Dubovik and King, 2000). These parameters are effective radius, size distribution (i.e. bimodal log-normal particles volume distribution), spectral SSA, and RI (real and imaginary parts). The impact of fires on these parameters can be estimated using the information of air masses transport by identifying the date when observed over Kyiv aerosols were transported from active fires regions. And then by comparing these data with observations when aerosols had different origin. In the

following, we compare those properties as averages over periods characterizing the fires strength and their influence on the time evolution of the Kyiv-site AOD, as described above. During the first period between June 1-26, the number of active fires in the considered area (40–65°N and 10–60°E, see Fig. 2) remained low. During the second period from July 18 to August 14 the fire count increased largely. The third period comprise the following three days when highest AOD values were observed (August 15–17). Partly data are also shown averaged over August 18–September 7, a period when the fire count significantly decreased.

The fires impact on aerosols size from AERONET sun photometer observations can be estimated by knowing the correlation between the aerosols effective radius and AOD (Fig. 6a) and size distribution of the aerosol particles in the total atmospheric column (Fig. 6b). The correlation coefficient for the fine mode is about 0.65, for the coarse mode only about 0.14. Bimodal volume distributions, inferred according Dubovik and King (2000) and averaged over the four aforementioned periods, clearly show that the fine mode fraction of aerosols is more sensitive to the fires strength when transported via similar pathways. In the period when most fires burned (July 18–August 14) the volume distribution of both modes increased by about 30-40%. In the following three days (August 15–17), when maximum AODs were observed (Fig. 4a,b), only the fine mode increased further by more than factor 2. This is an overall increase, compared to the earlier period with less fires activity (June 1–26), of almost about factor 4. Consistently, after August 18, when the atmosphere over Kyiv was cleaned again, aerosols sizes in both modes were even smaller than during earlier periods, indicating to be returned similar to the summer-time natural background level.

The dependence of SSA in the visible and near-infrared on the fires intensity and aerosol load over Kyiv is obvious from Fig. 6c by reduced values during the more intense fire period between July 18 and August 14. Most probably, these changes of SSA were caused by increase of soot content in the air, which was transported from the fires. Increased absorption of aerosol particles in the long-wave part of spectra is seen in the slope of the SSA spectral dependence, which becomes steeper. This holds true also during the three days when the highest AODs have been observed on August 15–17, although multiple light scattering effects in the dense aerosol layers lead to generally larger SSA values, on about the same level as during the period when less fires burned in June 2010 (multiple light scattering is not fully taken into account in the AERONET inversion algorithm). Because SSA of particles is defined by their complex RI, it explains similarities in spectral changes of SSA and real RI and also spectral changes of imaginary RI (Fig. 6d), which describes absorption properties of particles. The RI spectral dependence, however, is less pronounced than for SSA, but multiple light-scattering likely affects the imaginary part only. More detailed values of SSA and complex RI that were defined by measurements at Kyiv AERONET site during summer 2010 are given in Table 3, showing the daily averaged SSA as well as real and imaginary RI for 440 and 870 nm, Level 2.0 from AERONET database.

3.3 Using satellite data for estimating wildfires' influence on aerosols pollution over Ukraine

In order to estimate air pollution caused by wildfire aerosols we apply AOD parameter from the satellite instruments MODIS (on board Terra and Aqua) and CALIOP (on board CALIPSO). In Section 3.3.1 we compare the AOD derived from MODIS with collocated AERONET measurements performed over Kyiv site (as described in Sec. 3.2) and analyze the aerosols effect on air pollution over Ukraine. In Section 3.3.2 we compare AOD between MODIS and CALIOP for regions outside Kyiv and

Atmos. Meas. Tech. Discuss., https://doi.org/10.5194/amt-2017-336
Manuscript under review for journal Atmos. Meas. Tech.
Discussion started: 12 October 2017

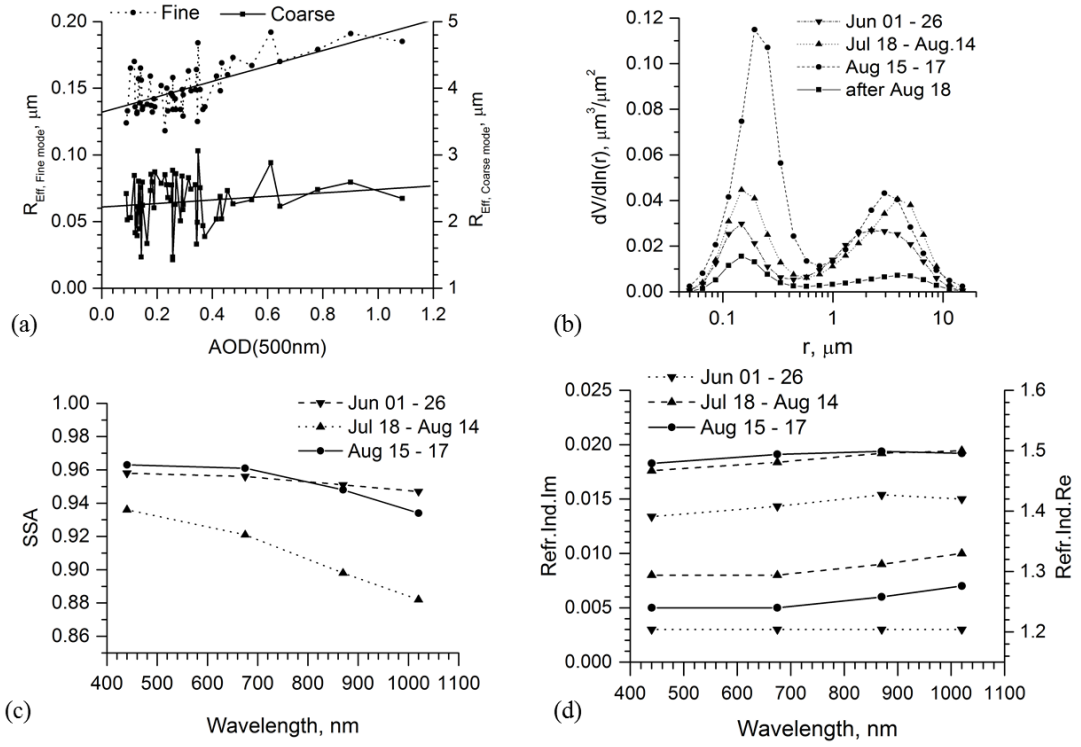

Figure 6. Aerosol particles microphysical properties from AERONET measurements at Kyiv site during summer 2010: a – particles effective radius versus AOD for fine (left axis, bottom curves) and coarse (right axis, top curves) modes averaged during 3 periods; b – particles size distribution averaged during 4 periods; c – spectral SSA; d – spectral refractive index, – real (right axis, top curves) and imaginary (left axis, bottom curves) parts averaged during 3 periods.

provide detailed analysis of CALIOP aerosols profiles over Ukraine within summer 2010. Comparison between CALIOP and AERONET was not performed because of lack of available collocations.

To link atmospheric pollution caused by biomass burning aerosols with fires activity, AOD variations and changes of weather conditions we divided summer 2010 into 3 main periods: pre-fires, active fires, and post-fires. These periods were distinguished according to characteristics of the spatio-temporal evolution of MODIS FRP (Sec. 2) and AOD 500 nm over the Kyiv AERONET site, together with an analysis of air mass transport to Kyiv from the HYSPLIT model.

Although a steady transport of air masses from regions of ETR, where fires burned, to Eastern Europe, including Ukraine, established only from approximately July 10 and both number and FRP during the following week were still relatively low. Consequently, the AOD over Kyiv did not increase significantly and remained on about the same level as during June and the beginning of July. Both fires activity over Eastern Europe and averaged AOD over Kyiv started to increase after reaching an

Atmos. Meas. Tech. Discuss., https://doi.org/10.5194/amt-2017-336
Manuscript under review for journal Atmos. Meas. Tech.
Discussion started: 12 October 2017

Atmospheric Measurement Techniques Discussions

Table 3. Aerosol particles microphysical properties from AERONET measurements at Kyiv site during summer of 2010 (SSA – Single Scattetring Albedo; Re, Im – real and imaginary parts of refractive index).

Date	SSA		R Index				Observations,
	440nm	870nm	Re440nm	Im440nm	Re870nm	Im870nm	number/day
1	2	3	4	5	6	7	8
09.06.2010	0.952	0.922	1.379	0.0059	1.383	0.0054	1
12.06.2010	0.947	0.928	1.347	0.0029	1.414	0.0043	2
13.06.2010	0.969	0.974	1.356	0.0020	1.414	0.0015	3
14.06.2010	0.965	0.978	1.483	0.0022	1.497	0.0015	1
30.06.2010	0.916	0.908	1.498	0.0082	1.521	0.0066	1
10.07.2010	0.941	0.891	1.367	0.0077	1.388	0.0097	1
19.07.2010	0.933	0.867	1.427	0.0081	1.460	0.0112	4
20.07.2010	0.947	0.900	1.398	0.0061	1.437	0.0075	2
31.07.2010	0.943	0.892	1.409	0.0073	1.430	0.0086	3
02.08.2010	0.941	0.945	1.521	0.0064	1.552	0.0051	4
05.08.2010	0.939	0.917	1.490	0.0060	1.532	0.0058	1
07.08.2010	0.940	0.916	1.505	0.0082	1.532	0.0089	8
08.08.2010	0.916	0.886	1.514	0.0091	1.556	0.0092	4
10.08.2010	0.928	0.869	1.475	0.0105	1.500	0.0156	3
11.08.2010	0.942	0.897	1.464	0.0082	1.485	0.0114	8
12.08.2010	0.943	0.905	1.498	0.0076	1.516	0.0096	3
13.08.2010	0.932	0.884	1.478	0.0087	1.511	0.0116	10
14.08.2010	0.939	0.894	1.491	0.0080	1.524	0.0113	3
15.08.2010	0.964	0.953	1.517	0.0056	1.527	0.0059	8
16.08.2010	0.965	0.946	1.493	0.0056	1.508	0.0071	10

intermediate minimum on July 15–16. On July 18, AOD 500 nm was approximately similar to its average over three previous weeks. Therefore, we define this time span from June 1 to July 18 as the pre-fires period.

For the following four weeks, the averaged AOD as well as the number and intensity of fires increased continuously over investigated region. Thus, the time span from July 19 to August 18 is considered as active fires period. On August 18 weather conditions started to change rapidly, leading to a significant AOD decrease over Kyiv. These conditions define post-fires period from August 19–31.

Atmos. Meas. Tech. Discuss., https://doi.org/10.5194/amt-2017-336
Manuscript under review for journal Atmos. Meas. Tech.
Discussion started: 12 October 2017

3.3.1 Using MODIS data.

MODIS and AERONET Kyiv site data comparison

Widely used procedure of MODIS AOD data validation by AERONET sunphotometers technique is stated in many publications, such as (Ichoku et al., 2002; Remer et al., 2005, 2008; Levy et al., 2010). In our analysis MODIS Collection 5 data are examined for potential regional peculiarities by means of comparison with relevant AERONET data and comparison slightly differs from the procedure used by Ichoku et al. (2002). We used MODIS image pixels containing Kyiv AERONET site computing only distances and azimuths angles between centers of each pixel of image's granule and AERONET site using coordinates of these points and determining the minimum of the distance set. MODIS AOD averaged over the pixels area centered on the Kyiv AERONET site are used to compare with AERONET AOD. This simplification of Ichoku et al. (2002) procedure is acceptable because MODIS images of land areas do not exceed an area of 50x50 km, which is significantly less than characteristic dimension of inhomogeneities in the spatial distribution of aerosols in the atmosphere (Anderson et al., 2003). In addition, we chose only one AERONET AOD measurement performed at time closest to the satellite measurement ($\pm$30 min). AERONET AOD 550 nm were interpolated by Angstrom equation using AE determined by AERONET algorithm at spectral interval 440–675 nm.

However, to estimate effects of possible irregularities in aerosol spatial distribution MODIS AOD 550 nm have been determined by three algorithms. 1) Choosing only one pixel closest to the AERONET site, with the distance between pixel center and AERONET station not exceeding 10-12 km. On average those pixels size is approximately 10 km $\times$ 10 km. It ensures that we compare AOD obtained at the same air mass. During June–August 2010 such events were found: 29 for Aqua and 36 for Terra. And the time span between sunphotometer and MODIS/Terra measurements exceeded 10 min at 4 cases whereas for MODIS/Aqua it happened one time only. 2) 3x3 pixels were selected from the MODIS dataset, with Kyiv AERONET site in the central pixel. The area averaging in this case is equal to approximately 30 km $\times$ 30 km. During three summer months of 2010 we found 38 events for Aqua and 40 for Terra, the time span between sunphotometer and MODIS/Terra measurements exceeded 10 min in 6 cases and for MODIS/Aqua in 7 ones. 3) 5x5 pixels were selected from MODIS dataset with Kyiv AERONET site in the central pixel, the area averaging was equal to approximately 50km $\times$ 50 km. This case corresponds to area size analysed by Ichoku et al. (2002). During the three summer months 2010 we found 39 events for Aqua and 40 for Terra (the same practically as in previous case), the time span between sunphotometer and MODIS/Aqua measurements exceeded 10 min in 8 cases and for MODIS/Terra in 7 cases. Unfortunately, we did not find MODIS data suitable for comparison with AERONET during post-fires period (i.e. after August 18). Comparisons were approximated by the straight-line equation with coefficients determined by least-square technique. It was assumed that random AOD measured by ground-based and satellite instruments are comparable and normally distributed. Linear regression coefficients, correlation coefficients and standard deviations of the points from regression line were computed for three cases: 1) all AOD 550 nm data for all three summer months; 2) for pre-fires period only; 3) for active fires period only. Results of this analysis is presented in Table 4.

Atmos. Meas. Tech. Discuss., https://doi.org/10.5194/amt-2017-336
Manuscript under review for journal Atmos. Meas. Tech.
Discussion started: 12 October 2017

Atmospheric Measurement Techniques Discussions

Table 4. Coefficients of Linear regression equation connecting AOD 550 nm determined for each of three spatial scales from MODIS and ground-based sunphotometers measurements: AOD_{MODIS} = a + b×AOD$_{Sph}$. Other parameters: R – Pearson's correlation coefficient; SD – standard deviation of the points from regression line; N – number of data used.

Area/	Aqua			Terra		
Period	10x10 km^2	20x20 km^2	30x30 km^2	10x10 km^2	20x20 km^2	30x30 km^2
All	a=−0.05±0.02	a=−0.06±0.02	a=−0.09±0.02	a=−0.08±0.02	a=−0.08±0.01	a=−0.11±0.01
Months	b=1.19±0.07	b=1.19±0.06	b=1.20±0.06	b=1.27±0.05	b=1.25±0.04	b=1.26±0.04
	R= 0.96	R=0.95	R=0.96	R=0.97	R=0.98	R=0.98
	SD=0.07	SD=0.08	SD=0.07	SD=0.06	SD=0.04	SD=0.05
	N=29	N=38	N=39	N=36	N=40	N=40
Pre-Fires	a=0.002±0.004	a=0.03±0.04	a=0.004±0.03	a=−0.09±0.04	a=−0.07±0.03	a=−0.08±0.03
	b=0.86±0.20	b=0.70±0.17	b=0.70±0.15	b=1.35±0.20	b=1.20±0.15	b=1.14±0.13
	R=0.81	R=0.73	R=0.78	R=0.89	R=0.91	R=0.92
	SD=0.07	SD=0.07	SD=0.06	SD=0.05	SD=0.05	SD=0.04
	N=12	N=16	N=16	N=14	N=16	N=16
Fires	a=−0.07±0.04	a=−0.09±0.04	a=−0.125±0.035	a=−0.10±0.03	a=−0.11±0.02	a=−0.15±0.03
	b=1.24±0.10	b=1.26±0.09	b=1.28±0.075	b=1.31±0.07	b=1.30±0.05	b=1.33±0.06
	R=0.96	R=0.96	R=0.97	R=0.97	R=0.99	R=0.98
	SD=0.08	SD=0.08	SD=0.07	SD=0.07	SD=0.04	SD=0.06
	N=16	N=20	N=21	N=19	N=21	N=21

Table 5. Statistics of matching between MODIS and sunphotometer AOD 550 nm in specified bounds during summer 2010 over Kyiv AERONET site: Abs(AOD_{MODIS} - $AOD_{Sph} \leq \pm(0.05 + 0.15\times$AOD$_{Sph})$).

Percentage/Number of cases						
Area/	Aqua			Terra		
Period	10x10km^2	20x20km^2	30x30km^2	10x10km^2	20x20km^2	30x30km^2
Pre-fires	75% / 12	81% / 16	81% / 16	71% / 14	81% / 16	69% / 16
Fires	81% / 16	90% / 20	81% / 21	79% / 19	86% / 21	81% / 21

We found that the differences AOD_{MODIS} - AOD$_{Sph}$ in most cases were within $\pm(0.05 + 0.15 \times AOD_{Sph})$ determined over land on a global scale for MODIS Collection 5 data, confirming Remer et al. (2008) and Levy et al. (2010). A statistical analysis for pre- and active fires periods is presented in Table 5.

Pearson's correlation coefficients (R) in Table 4 indicate functional relations between the AOD from AERONET and MODIS in all cases. Also, R for Terra data are higher in all cases than Aqua. Lower R during pre-fires period are explained by larger uncertainties of AOD estimated from both MODIS and AERONET, when aerosols load is low. Generally, our regression analysis is in good agreement with results of global analysis by Remer et al. (2008); Levy et al. (2010). This indicates that the

Atmos. Meas. Tech. Discuss., https://doi.org/10.5194/amt-2017-336
Manuscript under review for journal Atmos. Meas. Tech.
Discussion started: 12 October 2017

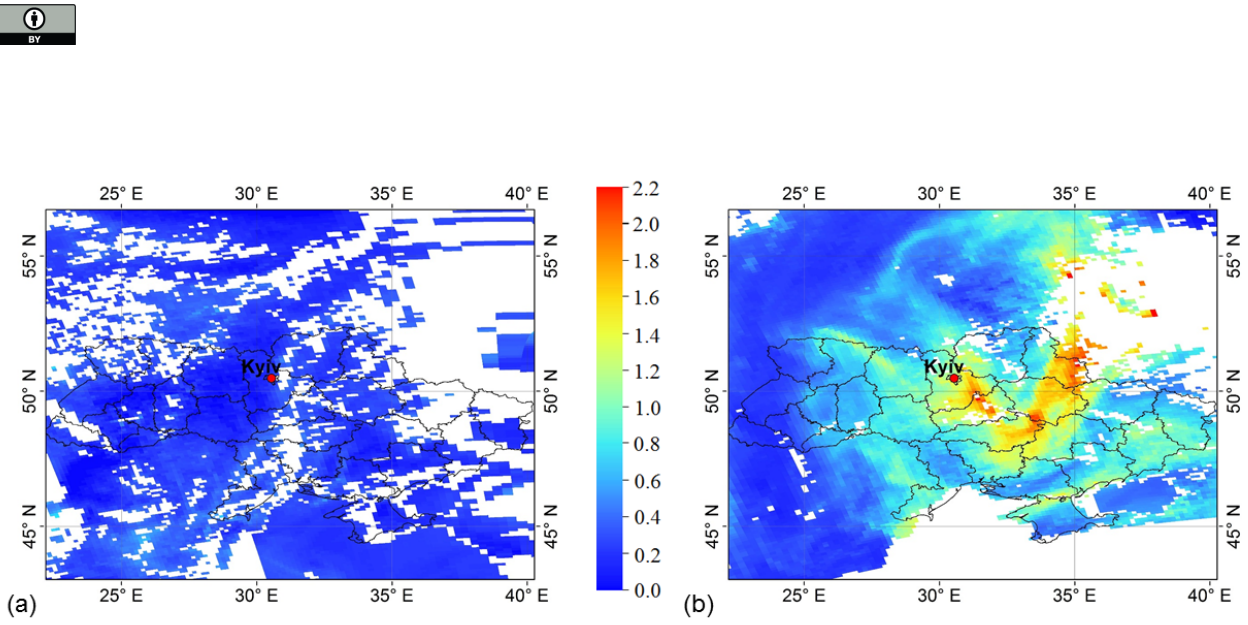

Figure 7. AOD 550 nm distribution from MODIS/Aqua measurements on July 17 (a) and August 15 (b)

MODIS algorithm interprets aerosols over Kyiv in the same manner as AERONET. Thus, we assume that both MODIS/Aqua and Terra correctly represent the content of aerosols in the atmosphere over Ukraine for summer 2010 within measurements uncertainties.

Estimations of aerosols pollution over Ukraine using MODIS.

From the AOD 550 nm distributions obtained from the MODIS Aqua and Terra Level 2 Collection 051 Optical Depth Land And Ocean product, the influence of aerosol pollution in Ukraine becomes obvious. For example, Fig. 7 shows maps for the region 40-60°N and 22.5-40°E of MODIS/Aqua data for those two days when the aerosols load over the Kyiv AERONET site was lowest (a, July 17) and highest (b, August 15).

Analysis of data for 7 days (June 6 and 7 from MODIS/Terra and June 8 from Aqua; July 14 and 17 from Aqua, July 15 from Terra; August 23 from Terra) with low AOD over Kyiv site and for 3 days with maximum AOD (August 15–17) showed the following: On low pollution days the AOD 550 nm is homogeneously distributed in the analyzed region, with values not exceeding 0.5. In the high pollution case, the spatial AOD distribution distinctly differs. Highest pollution is found over north-eastern and central regions of Ukraine, values reached a level of 2 and higher. This AOD distribution map (Fig. 7b) resembles fairly well our air mass back trajectory calculations to Kyiv in the altitude range 0.5–3 km for August 15 (see Fig. 3, Sect 3.1). Fig.7b highlights the importance on the availability of satellite observations for estimating air pollution over larger and remote regions, that clearly cannot be deduced from single site's ground-based measurements, as it is the case in Ukraine so far/right now.

Atmos. Meas. Tech. Discuss., https://doi.org/10.5194/amt-2017-336
Manuscript under review for journal Atmos. Meas. Tech.
Discussion started: 12 October 2017

3.3.2 Using CALIOP data

Using CALIOP AOD to study spatio-temporal distribution of aerosols and its validation by ground-based AERONET observations is challenging due to different measurement characteristics of both instruments. CALIOP lidar provides only fragmentary data on aerosols along CALIPSO satellite's ground track, because of the small size of light beam (with diameter approximately 70 m) and cloudy conditions that frequently occurred. Due to orbital period of 98 minutes, ground tracks of satellite consecutive passages of certain latitude are shifted 24.5°to the west, thus its spatio-temporal coverage is rather sparse. During three summer months in 2010 we did not find CALIOP - AERONET coincident measurements over Kyiv, but one: the closest CALIPSO ground track was 60 km east from Kyiv AERONET site, hence, not matching the selection criteria (40 km) according to (Omar et al., 2013) for CALIOP-AERONET comparisons.

Therefore, in this study we estimated CALIOP AOD using MODIS/Aqua AOD since both satellites orbits are in A-Train afternoon constellation (http://atrain.nasa.gov/). Relative positions of CALIPSO and Aqua satellites in the A-Train provide great number of practically simultaneous measurements with the time span of 2 minutes, while the spatial difference is only about 10 km. We applied MODIS Aqua Level 2 Collection 051 Optical_Depth_Land_And_Ocean product AOD 550 nm and CALIPSO CloudAerosol Layer Product- AOD 532 nm, together with Aerosols Profile Product Level 2.0 Version 3.01 and 3.02 (Winker et al., 2009, 2010).

Each granule of MODIS data consists of consecutive scans across the satellite track. The footprint of CALIOP light beam on this granule looks like a sequence of points on the straight line passing close to the center of a granule. Each point represents the center of CALIOP dataset, averaged over 5-km and once or twice matches with one of the pixels of MODIS granule. To find these matches we calculated the distances and azimuth angles between the center of each 5-km segments of the CALIOP track and the center of each pixel in MODIS granule in the same manner as for MODIS-AERONET case (see above).

While comparing CALIOP AOD 532 nm and MODIS/Aqua AOD 550 nm, no corrections for potential spectral differences were applied. This yields to an estimated systematic bias in our AOD comparison of approximately 2–4% in the AE range between 0.5 to 1.0, thus, may be neglected in our cases, following Kittaka et al. (2011) . The two instruments comparison was performed in the same manner as our MODIS-AERONET comparison (see Section 3.3.1), in similar temporal and spatial scales.

Linear regression parameters (Table 6) indicate a weak correlation between CALIOP and MODIS AOD during pre-fires period (i.e. low AOD), with $0{,}16 \leq R \leq 0{,}25$, and stronger correlation during period of active fires with $R \approx 0{,}6$. A direct comparison of the two AOD datasets is given in Table 7, averaged over pre-fires period (time span 1, June 5–July 17), active fires period (time span 2, July 19–August 13), and for a single day, when one of the highest AOD was measured over Kyiv AERONET site (time span 3, August 17). CALIOP and MODIS AODs are very similar during time span 1. During time span 2, when aerosols from active fires influenced the atmosphere over Ukraine, the MODIS AOD exceeded those measured by CALIOP by 7–16%, depending on the spatial scale of the MODIS average. The smallest difference is found in 50 km × 50 km average, and the largest – in 10 km ×10 km average. But in case of largest aerosols loading during time span 3, AOD CALIOP exceeds that of MODIS by 7–12% and the differences are maximum at smallest averaging area and vice versa.

Atmos. Meas. Tech. Discuss., https://doi.org/10.5194/amt-2017-336
Manuscript under review for journal Atmos. Meas. Tech.
Discussion started: 12 October 2017

Atmospheric Measurement Techniques Discussions

Table 6. Coefficients of linear regression equation connecting AOD 550 nm determined for each of two spatial scales from MODIS and CALIOP (532 nm) measurements: AOD_{MODIS} = a + b×AOD$_{CAL}$.

Area/ Period	10x10km^2	30x30km^2	50x50km^2
Pre-fires	a=0.09±0.004	a=0.1±0.003	a=0.1±0.004
	b=0.19±0.02	b=0.17±0.02	b=0.15±0.02
	R=0.25	R=0.20	R=0.16
	SD=0.09	SD=0.10	SD=0.10
	N=1106	N=1425	N=1491
Fires	a=0.05±0.009	a=0.06±0.008	a=0.04±0.008
	b=0.72±0.025	b=0.72±0.025	b=0.81±0.026
	R=0.62	R=0.58	R=0.61
	SD=0.19	SD=0.20	SD=0.19
	N=1325	N=1625	N=1675

Table 7. Comparison the CALIOP and MODIS AOD for three time span during the summer 2010.

Period	Averaging area	AOD CALIOP (532 nm)	AOD MODIS (550 nm)
Time span 1	10x10km^2	0.115	0.127
	30x30km^2	0.121	0.125
	50x50km^2	0.122	0.118
Time span 2	10x10km^2	0.205	0.240
	30x30km^2	0.208	0.233
	50x50km^2	0.206	0.220
Time span 3	10x10km^2	0.723	0.671
	30x30km^2	0.715	0.642
	50x50km^2	0.715	0.631

Such differences between MODIS and CALIOP data can be explained by different independent measurements techniques, algorithms, and by uncertainties of CALIOP daytime measurements. In this paper we do not analyze peculiarities of MODIS and CALIOP data and reasons of their discrepancies, more detailed analysis can be found in Kittaka et al. (2011); Redemann et al. (2012).

Taking also into account uncertainties of both day- and nighttime CALIOP measurements, it's AOD reasonably captures air pollution from wildfire aerosols. Most CALIOP data were obtained during night and have a higher fidelity than daytime measurements (Omar et al., 2013). Up to now CALIOP is the only instrument that provides data on nocturnal pollution of the atmosphere by aerosols. Due to its sparse coverage over investigated regions, the data product can be used only to roughly estimate severeness of pollution over longer periods. This is well illustrated in Fig. 8, exemplary showing all day- and night-

Atmos. Meas. Tech. Discuss., https://doi.org/10.5194/amt-2017-336
Manuscript under review for journal Atmos. Meas. Tech.
Discussion started: 12 October 2017

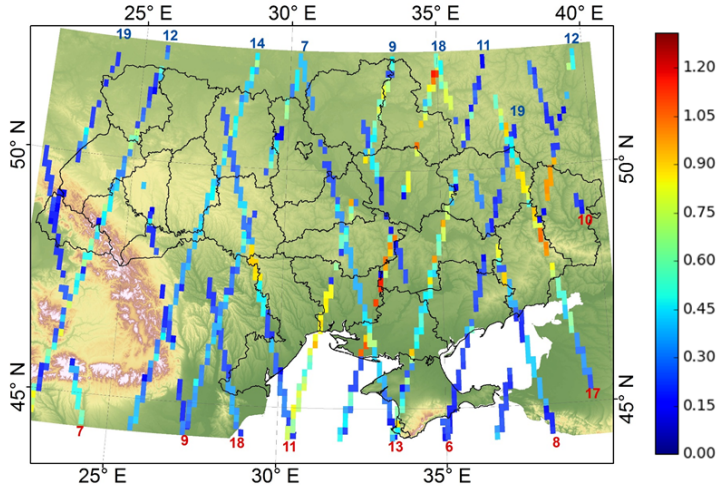

Figure 8. AOD 532 nm distribution over Ukraine from CALIOP measurements during the 16-day period from August 4 to 19, 2010. Red numbers at the bottom of the map indicate dates of each daytime track running to north-west and blue numbers at the top of the map indicate the date of each nocturnal track running to south-west.

time AOD measurements during a 16-days period from August 4 to 19, 2010 that corresponds to one repeating cycle of the instrument. The tracks, that are oriented from northeast to southwest correspond to nocturnal measurements and those, oriented from southeast to northwest correspond to daytime measurements. Fig.8 shows distinct pattern of aerosols pollution, except over western Ukraine, mostly during 11-18 August with AOD values exceeding 0.5. This is in good agreement with MODIS observations on August 15 as shown in Fig. 7b. During these days weather conditions were stable and did not changed much. For both instruments higher values of 1–1.2 are seen over central and eastern Ukraine.

The CALIOP measured AOD 532 nm over Ukraine and surrounding territories ranged approximately from 0 to 0.5 during first part of the summer 2010 (June 1 – July 18), when number and intensity of fires were still low. CALIOP confirms that with July 19 aerosols content in the atmosphere significantly increased, corresponding to fires activity. During August 4–17 over certain regions of Ukraine, mainly east and south, observed AOD 532 nm was around 1. After August 17 number and intensity of fires, thus, aerosols content decreased dramatically and AOD distribution returned to pre-fires values. In general, these results are in agreement with our findings from MODIS.

CALIOP measurements also provide information about the vertical distributions of aerosols extinction at 532 nm from the Cloud&Aerosol Profile Product Level 2.0 Version 3.01 and 3.02 (Young et al., 2013; Omar et al., 2013).The aerosol extinction is proportional to concentration of the aerosol particles along the light beam and extinction vertical profiles reveal vertical distribution of aerosols in the atmosphere column. Here, we analyzed profiles compiled for those sections of CALIOP ground tracks where the highest AOD 532 nm was measured. This selection leads to 58 profiles for 11 tracks we analysed for the period August 7–18, 2010. The corresponding AOD 532 nm ranged from 0.44 (on August 13 11:00:06) to 2.93 (on August 18 00:08:26). Among selected profiles, 37 on 7 ground tracks were nocturnal, and 21 profiles on 4 tracks were measured during

daytime. The profiles reveal that aerosols ranged from about 40 m to 6 km altitude. The vertical distributions varied significantly both during day- and nighttime and three types of profiles were identified. 1) The first type consists of profiles showing at least a single aerosols layer of some hundred meters thickness, located at about 1km altitude or higher. 2) The second type consists of profiles showing decreasing extinction coefficients with increasing altitude. 3) The third type is characterized by relatively high extinction values over comparably large altitude ranges, spanning several kilometers, without showing distinct maxima. Fig. 9 depicts corresponding profiles, exemplarily selected for those cases when the above mentioned features are well pronounced. All other cases are shown in the Supplementary material (Fig. S31-S88).

Aerosol extinction profile shown on Fig. 9a reveals vertical distribution of particles concentration at two points on daytime CALIOP trace of August 08, 2010 running through south-east of Ukraine (see Fig. 8). Distance between the points with coordinates 47.67°N, 36.96°E and 48.29°N, 36.71°E is approximately 70 km, AOD 532 nm at these points was 1.00 and 0.84 respectively. At these points almost all aerosols concentrate in a narrow layer at altitudes between 3.1 and 3.8 km (type 1 profile). Extinction profile shown on 9b was observed at some points on 320 km segment of CALIOP midnight track on August 11 between 48.81°N, 35.08°E (AOD = 1.58) and 46.11°N, 34.04°E (AOD = 0.99). Aerosols at these points located mainly in three thin layers with maximums at 0.3, 1.3, and 4.2 km. Considered track segment lies on distance 210–250 km westward from daytime track segment of August 8.

Our back trajectory suggests CALIOP observed the same air masses on both days at different measurement times. Daytime CALIOP track on August 11 runs over west regions of Ukraine. Peak aerosol load in terms of AOD 532 nm is found in south-west region of Ukraine, with values around 0.9 (Fig. 8). Here, the measured aerosols extinction profile is of type 2, showing a maximum at 300–350 m altitude and gradually decreases above, up to 5 km altitude (Fig. 9c).

CALIOP's nocturnal track on August 12 also runs over east of Ukraine, where the highest aerosols AOD 532 nm of about 1.0 is found approximately over Lugansk region (Fig 8). Over a track segment of about 80 km length, most of aerosol particles concentrated below 2 km altitude, with a maximum extinction coefficient at approximately 280 m. Another, less dense aerosol layer was observed also above between 3 to 4.5 km altitude (Fig.9d).

Five days later, on August 17, the instrument measured over the same region during daytime (Fig.8). But here, aerosols conditions were much more variable than on days before. In Fig. 9e and f we show two consecutively measured profiles with 15 sec time difference that corresponds to approximately 100 km distance between appropriate points. The maximum extinction coefficient of the profile, measured first (Fig. 9e), was located at about 220 m and above gradually decreases. On the second profile, the maximum extinction coefficient was found significantly higher, at approximately 1 km altitude (Fig. 9f). Below, extinction values indicate clean air with values not exceeding 0.3 km-1. In the two measurements the vertical extent of aerosol is about the same (about 3 km). The AOD of both profiles do not differ much and range from 0.92 to 1.0.

On August 18, the day when weather situation significantly changed, the extinction coefficient profile shows much higher variability (Fig.9g). The layer extents up to about 4 km. The analysed segment of CALIOP's nocturnal track had a length of about 360 km and is located between 52.28°N, 35.04°E and 49.33°N, 33.75°E. The track was westward oriented, relative to the daytime track on August 17. Relatively high extinction coefficients are found from near the surface up to about 2km. Although being highly variable, the vertical structure does not decline much until 3.8 km altitude, in contrast to other profiles discussed

before. The AOD 532 nm was significantly larger than measured before, equal to 1.46. As shown in the Supplementary, AOD values up to 2.93 were measured on this day (Fig. S84).

Finally wide range of the extinction coefficient variations has to be noted in the maximums of profiles. It ranges from some tenth to 8.5 km^{-1} in certain very dense plumes but the most frequent occurring value was approximately 1 km^{-1}.

Our CALIOP profile measurements reflect well the large diversity of aerosol layers in the region and period under review. Those structures, as lofting of highest pollution regions above ground, multiple layers or zones of relatively clean air, cannot be determined from vertically integrated observational parameter, like AOD, although other instrument's spatial sampling allows investigation on more coherent spatial structures.

4 Discussions and conclusions

Analysis of AOD measured by AERONET, MODIS and CALIOP, together with transport of air masses by application of back trajectories simulations, allowed estimating air pollution over Ukraine caused by exceptional wildfires in Eastern Europe during summer 2010. These fires were the biggest by area burned, the longest by duration and the most intense for the whole period of AERONET aerosols observations in Ukraine. On Kyiv AERONET site, these fires caused the highest AOD measured so far. However, analysis of the spatio-temporal variability of atmospheric pollution caused by aerosols from fires over above-mentioned territories was not done before.

In this research we used ground-based measurements from AERONET sites and data from satellite instruments MODIS (Aqua and Terra) and CALIOP (CALIPSO). The highest accuracy in such remote measurements is achieved by measuring spectral AOD with the AERONET sun-photometers and by solving inverse problem, which retrieves microphysical properties of aerosol particles (see section 2.1). These data were used as the standard for validation of satellite measurements that always have lower accuracy.

Since there were very few AERONET sites over investigated territories in summer 2010, we filled spatio-temporal gaps in the ground-based observations by applying satellite data. For this purpose we used measurements from MODIS on board the Terra and Aqua satellites because the wide field of view of this instrument (over 2 000 km) scans each location at least twice a day. Thus, we validated MODIS data by comparing with collocated AERONET measurements (section 3.3.1). Also, the algorithms of determination of aerosols optical properties from MODIS measurements are well developed and tested over ocean and land for different natural zones, also data quality is known (Remer et al., 2008; Levy et al., 2010). Our comparison over Kyiv in summer 2010 is in agreement with other studies, see Remer et al. (2008); Levy et al. (2010). The functional relation between the AOD measured by AERONET and MODIS over Kyiv (section 3.3.1, Table 4) suggests that the MODIS data product is reasonable for researched territory.

Analysis of spatio-temporal evolution of AOD obtained from CALIOP measurements was rather challenging task due to fragmentation of data and their high variability. Although AOD measurements from CALIOP have higher uncertainties in comparison with MODIS, the clear advantage is that they are also performed at night-time. Despite the sparse availability of CALIOP measurements for the time and regions we analysed, it was the only source of aerosols vertical distribution.

Atmos. Meas. Tech. Discuss., https://doi.org/10.5194/amt-2017-336
Manuscript under review for journal Atmos. Meas. Tech.
Discussion started: 12 October 2017

Spatial distribution of AOD from CALIOP measurements over Ukraine corresponds well with MODIS, with the correlation coefficient R = 0.6, see section 3.3.2, Table 6, 7. This is in agreement with Kittaka et al. (2011), who compared CALIOP Version 2 Aerosol Layer Product with MODIS Collection 5 and found only a small global mean bias in the CALIOP daytime AOD, relative to MODIS. On regional scale, biases of both signs were larger and varied with seasons. Additionally, over land this regional-seasonal bias was not larger than MODIS expected uncertainty. However, data presented in Table 7 show systematical differences between MODIS and CALIOP. Interestingly, in periods with moderate pollution the AOD from MODIS is larger than from CALIOP. But during the short period of highest pollution, i.e. August 15-17, 2010 the CALIOP AOD is larger. These peculiarities were also noticed in other studies. E.g. Ma et al. (2013) compared monthly mean gridded data and noted systematically higher CALIPSO AOD over other major biomass burning regions (such as South Africa) during fire seasons. One reason explaining these peculiarities may be found in the CALIOP Version 2 retrieval algorithm itself, because it retrieves aerosols extinction that is converted into AOD. According Kittaka et al. (2011), the CALIOP algorithm likely ignores tenuous aerosols, causing an underestimation of AOD compared to MODIS. Also, the height of aerosols layer's base may be detected at higher altitudes by CALIOP, leading to AOD underestimation (Kittaka et al., 2011). Main factors that determine data accuracy are uncertainties of instrument's calibration and the low signal-to-noise (STN) ratio for daytime measurements. That is why an algorithm is used to estimate the "lidar ratio" (the ratio of particle extinction to 180-degree backscatter) from the 532 nm backscatter and it is also the significant source of uncertainties in defining aerosols parameters by the algorithms of the corresponding inverse solution (Omar et al., 2009; Winker et al., 2009).

Taking into account atmospheric dynamics by applying back trajectories calculated with HYSPLIT for the range of altitudes up to 5 km allowed to relate the increase of observed aerosols abundance over AERONET sites in Eastern Europe with biomass burning in the particular territories of investigated region. To estimate the spatial extent of aerosols from wildfires in central parts of ETR and other regions of Eastern Europe, we analyzed data from AERONET sites and MODIS measurements in Eastern Europe during summer 2010. Observed increase of AOD at each of the 10 AERONET sites considered in this paper was caused by wildfires events. As discussed in section 3.1, by analysing back trajectories for the days with maximum AOD values, the air masses, which were transported to Belsk site (central Poland), Chisinau (Moldova), and Romania sites (Bucharest, Cluj-Napoca, Eforie) in the lower atmospheric layers up to 1.5 km, were passing areas with active fires, mainly throughout Ukraine and Moldova. Maximum AODs over other AERONET sites were caused by aerosols, that were transported with air masses along the anticyclone periphery over Russian Federation regions, where also intense forest fires burned.

Analysis of spatio-temporal distributions of fires number and intensities over Eastern Europe as well as our air mass back trajectory calculations led to the conclusion that most aerosols from forest fires in Russia were transported to Ukraine, and later to Belarus and Baltic countries, from around July 18 until August 18–19. This was the time of most intense fires in this region, which lasted from July 22 to August 18–19, 2010, corresponding to Witte et al. (2011). From analyzing spatio-temporal AOD distributions from MODIS and CALIOP we conclude that the fires had significant impact on the air quality above the whole territory of Ukraine. Most affected regions were the eastern, central and southern parts of the country.

CALIOP shows approximately the same aerosols content for day- and nighttime measurements (no distinct diurnal cycle) for all investigated periods over Ukraine, and is therefore in agreement with global analysis by Kittaka et al. (2011). In section

3.3.2 we showed vertical distributions of aerosols extinction measured by CALIOP for the territory of Ukraine, where high AOD values were observed during intense wildfires. We did not validate CALIOP data with ground-based measurements due to lack of collocations. In order to estimate the reliability of CALIOP data we used results of other authors obtained for similar situation. Chazette et al. (2010) performed a validation of CALIOP Version 2 daytime aerosol extinction product under low content of aerosols AOD 532 nm < 0.3 during a field experiment on April 28, 2006 over France with the ground-based and airborne lidars, also employing observations from the CIMEL sunphotometer and the satellite instruments MODIS and SEVIRI. In their works measurement sites were mainly located in urban areas where rather complex aerosol compounds are expected. Chazette et al. (2010) showed that CALIOP provides high quality information on the structure of aerosol layers with AOD 532 nm < 0.3.

Kacenelenbogen et al. (2011) performed a validation of the CALIOP Version 2 and 3 daytime aerosol extinction product under conditions of high aerosols pollution (AERONET AOD 532 nm $\approx$ 0.71). They analyzed measurements of August 4, 2006 over territory of USA by applying data from lidar installed on aircraft, AERONET site, and from the MODIS, and POLDER instruments. Vertical profiles of aerosols extinction retrieved from CALIOP agree well with ground-based instruments, with significantly better agreement of CALIOP Version 3 data. The main differences are caused by the CALIOP extinction retrieval, which is insensitive to aerosols outside relatively thick layers (tenuous aerosols), in turn leading to an AOD underestimation. In summary, studies of the structure of aerosol layers on the atmosphere pollution over great urban areas using CALIOP observations appear feasible when significant pollution occurs. In our study, we analyzed CALIOP data for events of high aerosols content only, and we assume that results presented in section 3.3.2 correctly represent vertical distributions of aerosols over Ukraine during active fires and when aerosols were transported in the lower 5 km of the atmosphere.

In section 3.2 we provided evidence of the fires impact on microphysical characteristics of aerosol particles according to measurements of Kyiv AERONET site. Similar conclusions were also provided by other studies (Chubarova et al., 2012; Witte et al., 2011; Péré et al., 2014), who analyzed the variability of microphysical aerosols properties, like SSA and RI, under the impact of wildfires during summer 2010 over Eastern Europe. Chubarova et al., (2012) analyzed those effects for Moscow and suburbs from AERONET measurements. Witte et al. (2011) provides averaged estimations of SSA according to satellite (OMI) and ground-based (AERONET) measurements during intense fires (July 22-August 18, 2010) for all Eastern Europe including Ukraine. Péré et al. (2014) analyzed SSA and RI, received from POLDER and AERONET measurements, and compared to chemical-transport model CHIMERE data, mainly for Moscow region.

In this study, we analyze in some detail microphysical properties retrieved from measurements at Kyiv AERONET site only. The influence of fires resulted in an increase of the relative content of the fine mode in particles size distribution, accompanied with a decrease of both their effective radius and SSA. Therefore, aerosols absorptive capacity increased, and changes of spectral properties of SSA and RI real and imaginary parts were observed (Fig. 6). Microphysical properties of aerosol particles over Kyiv under the influence of intense fires correspond well with general characteristics of biomass burning and polluted continental aerosols, as derived from AERONET sun-photometers measurements (Dubovik et al., 2002; Omar et al., 2005, 2009). Both aerosol types are mainly spherical, their size distributions are dominated by the fine mode, and they are both moderately absorbing. In particular these types of aerosols are not separated in the algorithms of satellite measurements.

Atmos. Meas. Tech. Discuss., https://doi.org/10.5194/amt-2017-336
Manuscript under review for journal Atmos. Meas. Tech.
Discussion started: 12 October 2017

Particularly the CALIOP algorithm exploits the probability that smoke aerosols are likely to be lofted, leaving unresolved cases where the smoke is in the boundary layer. Because the main objective of the algorithm is to select an appropriate lidar ratio, a potential misinterpretation of these two types has no effect on the retrieved extinction because both types are assigned the same aerosol extinction-to-backscatter ratio of about 70 sr (Omar et al., 2009).

Witte et al. (2011) showed AOD 550 nm measured by MODIS and SSA (388 nm) measured by OMI, averaged over the active fire period from July 22 to August 18, 2010 for domains covering territory of Ukraine and neighboring areas (domain 9: 45–52°N and 23–33; domain 10: 45–52°N and 33–43°E). The SSA is retrieved on assumption that black carbon and organic components dominate in aerosols, thus SSA can be overestimated for urban areas, and the vertical aerosols distribution has the shape of Gaussian with the maximum at the altitude of 3 km. Our analysis of vertical profiles of extinction coefficient for the cases of significant aerosols pollution indicates that this is assumption is unrealistic. Witte et al. (2011) found SSA = 0.98±0.02 (domain 9) that are much higher than our data received over Kyiv for the same time period (Fig. 6c). Nevertheless Witte's conclusion "... Decreased OMI SSA (increased aerosol absorption) is consistent with increased smoke", agrees well with our results. And Witte's AOD 550 nm of 0.34±0.6 is representative for the investigated area, but obviously too low in comparison with mean value for Kyiv (0.45). For eastern Ukraine (domain 10), Witte et al. (2011) shows SSA = 0.97±0.02 and AOD 550 nm = 0.44±0.26, that are matching well with our conclusion that fires caused the largest and most significant impact on this part of Ukraine. For comparison: average values at Kyiv AERONET site for SSA (440 nm) in pre-fires period were equal to 0.96 and 0.94 during active fires; for SSA (870 nm) were 0.95 and 0.91 respectively (Fig. 6c).

Chubarova et al. (2012) estimated the impact of forest fires during summer 2010 on aerosols properties over Moscow according to AERONET measurements by comparing averages over periods of active fires and for the decade 2001–2010. During fire periods both the relative content of fine mode particles and the geometric mean radius of their size distributions significantly increased. This is in agreement with our results and conclusions of the other authors for different geographic regions (Dubovik et al., 2002; Eck et al., 2009). Also, Chubarova et al. (2012) found an increase in the real part of the refractive indices and a decrease of imaginary parts. This results in larger SSA values in the visible and infrared spectrum. This is contradictory to our results (Fig. 6c,d), but agrees with Eck et al. (2009), where this relationship is explained by increase of particles size, that results in increasing the total reflectance of particles in the atmospheric column.

Finally, as the measurements in the two above-mentioned studies were performed close to the sources of combustion, the transport of air from the burning cells to Kyiv which took a significant amount of time, resulted in the transformation of the aerosols properties and the composition of particles.

Data availability. The AERONET dataset of AOD, AE, aerosols size distribution, SSA and RI are available upon special data request on https://aeronet.gsfc.nasa.gov. MODIS AOD dataset (Terra and Aqua) are available upon request from the authors. MODIS data of spatio-temporal fires distribution are available on https://lance.modaps.eosdis.nasa.gov/cgi-bin/imagery/firemaps.cgi?period=2010221-2010230. CALIOP dataset of Level 2 Cloud and Aerosol Layer and Profile products V 3.01 and 3.02 are available upon request from the authors. HYSPLIT results are available upon request from the authors.

Competing interests. The authors declare that they have no conflict of interest.

Acknowledgements. This publication includes results of the research that is performed in Astronomical observatory of Taras Shevchenko National university of Kyiv, project 16Ф023-01, funded by Ministry of Education and Science of Ukraine. Parts of the research has been funded by the University and State of Bremen.

We thank the (PI investigators) and their staff for establishing and maintaining the Minsk, Moscow, Toravere, Belsk, Chisinau, Cluj-Napoca, Bucharest, Eforie, Kyiv and Sevastopol AERONET sites used in this investigation.

References

Anderson, T. L., Charlson, R. J., Winker, D. M., Ogren, J. A., and Holmén, K.: Mesoscale Variations of Tropospheric Aerosols, Journal of Atmospheric Sciences, 60, 119–136, doi:10.1175/1520-0469(2003)060<0119:MVOTA>2.0.CO;2, 2003.

Barnaba, F., Angelini, F., Curci, G., and Gobbi, G. P.: An important fingerprint of wildfires on the European aerosol load, Atmospheric Chemistry and Physics, 11, 10 487–10 501, doi:10.5194/acp-11-10487-2011, http://www.atmos-chem-phys.net/11/10487/2011/, 2011.

Bovchaliuk, A., Milinevsky, G., Danylevsky, V., Goloub, P., Dubovik, O., Holdak, A., Ducos, F., and Sosonkin, M.: Variability of aerosol properties over Eastern Europe observed from ground and satellites in the period from 2003 to 2011, Atmospheric Chemistry and Physics, 13, 6587–6602, doi:10.5194/acp-13-6587-2013, http://www.atmos-chem-phys.net/13/6587/2013/, 2013.

Bowman, K. P., Lin, J. C., Stohl, A., Draxler, R., Konopka, P., Andrews, A., and Brunner, D.: Input Data Requirements for Lagrangian Trajectory Models, Bulletin of the American Meteorological Society, 94, 1051–1058, doi:10.1175/BAMS-D-12-00076.1, http://dx.doi.org/10.1175/BAMS-D-12-00076.1, 2013.

Bréon, F.-M., Vermeulen, A., and Descloitres, J.: An evaluation of satellite aerosol products against sunphotometer measurements, Remote Sensing of Environment, 115, 3102 – 3111, doi:https://doi.org/10.1016/j.rse.2011.06.017, http://www.sciencedirect.com/science/article/pii/S0034425711002410, 2011.

Chazette, P., Raut, J.-C., Dulac, F., Berthier, S., Kim, S.-W., Royer, P., Sanak, J., Loaëc, S., and Grigaut-Desbrosses, H.: Simultaneous observations of lower tropospheric continental aerosols with a ground-based, an airborne, and the spaceborne CALIOP lidar system, Journal of Geophysical Research: Atmospheres, 115, n/a–n/a, doi:10.1029/2009JD012341, http://dx.doi.org/10.1029/2009JD012341, d00H31, 2010.

Chubarova, N., Nezval', Y., Sviridenkov, I., Smirnov, A., and Slutsker, I.: Smoke aerosol and its radiative effects during extreme fire event over Central Russia in summer 2010, Atmospheric Measurement Techniques, 5, 557–568, doi:10.5194/amt-5-557-2012, 2012.

Crutzen, P. J. and Andreae, M. O.: Biomass Burning in the Tropics: Impact on Atmospheric Chemistry and Biogeochemical Cycles, Science, 250, 1669–1678, doi:10.1126/science.250.4988.1669, http://science.sciencemag.org/content/250/4988/1669, 1990.

Danylevsky, V., Ivchenko, V., Milinevsky, G., Grytsai, A., Sosonkin, M., Goloub, P., Li, Z., and Dubovik, O.: Aerosol layer properties over Kyiv from AERONET/PHOTONS sunphotometer measurements during 2008–2009, International Journal of Remote Sensing, 32, 657–669, doi:10.1080/01431161.2010.517798, http://dx.doi.org/10.1080/01431161.2010.517798, 2011a.

Danylevsky, V., Ivchenko, V., Milinevsky, G., Sosonkin, M., Goloub, P., Li, Z., and Dubovik, O.: Atmosphere Aerosol Properties Measured with AERONET/PHOTONS Sun-Photometer over Kyiv During 2008–2009, pp. 285–294, Springer Netherlands, Dordrecht, doi:10.1007/978-90-481-9618-0_32, http://dx.doi.org/10.1007/978-90-481-9618-0_32, 2011b.

Davies, D. K., Ilavajhala, S., Wong, M. M., and Justice, C. O.: Fire Information for Resource Management System: Archiving and Distributing MODIS Active Fire Data, IEEE Transactions on Geoscience and Remote Sensing, 47, 72–79, doi:10.1109/TGRS.2008.2002076, 2009.

Draxler, R. R. and Hess, G. D.: An Overview of the HYSPLIT_4 modeling system for trajectories, dispersion and deposition, Aust. Met. Mag., 47, 295–308, 1998.

Dubovik, O. and King, M. D.: A flexible inversion algorithm for retrieval of aerosol optical properties from Sun and sky radiance measurements, Journal of Geophysical Research: Atmospheres, 105, 20 673–20 696, doi:10.1029/2000JD900282, http://dx.doi.org/10.1029/2000JD900282, 2000.

Dubovik, O., Smirnov, A., Holben, B. N., King, M. D., Kaufman, Y. J., Eck, T. F., and Slutsker, I.: Accuracy assessments of aerosol optical properties retrieved from Aerosol Robotic Network (AERONET) Sun and sky radiance measurements, Journal of Geophysical Research: Atmospheres, 105, 9791–9806, doi:10.1029/2000JD900040, http://dx.doi.org/10.1029/2000JD900040, 2000.

Dubovik, O., Holben, B., Eck, T. F., Smirnov, A., Kaufman, Y. J., King, M. D., Tanré, D., and Slutsker, I.: Variability of Absorption and Optical Properties of Key Aerosol Types Observed in Worldwide Locations, Journal of the Atmospheric Sciences, 59, 590–608, doi:10.1175/1520-0469(2002)059<0590:VOAAOP>2.0.CO;2, http://dx.doi.org/10.1175/1520-0469(2002)059<0590:VOAAOP>2.0.CO;2, 2002.

Eck, T. F., Holben, B. N., Reid, J. S., Sinyuk, A., Hyer, E. J., O'Neill, N. T., Shaw, G. E., Vande Castle, J. R., Chapin, F. S., Dubovik, O., Smirnov, A., Vermote, E., Schafer, J. S., Giles, D., Slutsker, I., Sorokine, M., and Newcomb, W. W.: Optical properties of boreal region biomass burning aerosols in central Alaska and seasonal variation of aerosol optical depth at an Arctic coastal site, Journal of Geophysical Research: Atmospheres, 114, n/a–n/a, doi:10.1029/2008JD010870, http://dx.doi.org/10.1029/2008JD010870, d11201, 2009.

Holben, B., Eck, T., Slutsker, I., Tanré, D., Buis, J., Setzer, A., Vermote, E., Reagan, J., Kaufman, Y., Nakajima, T., Lavenu, F., Jankowiak, I., and Smirnov, A.: AERONET—A Federated Instrument Network and Data Archive for Aerosol Characterization, Remote Sensing of Environment, 66, 1 – 16, doi:https://doi.org/10.1016/S0034-4257(98)00031-5, http://www.sciencedirect.com/science/article/pii/S0034425798000315, 1998.

Hunt, W. H., Winker, D. M., Vaughan, M. A., Powell, K. A., Lucker, P. L., and Weimer, C.: CALIPSO Lidar Description and Performance Assessment, Journal of Atmospheric and Oceanic Technology, 26, 1214–1228, doi:10.1175/2009JTECHA1223.1, http://dx.doi.org/10.1175/2009JTECHA1223.1, 2009.

Ichoku, C., Chu, D. A., Mattoo, S., Kaufman, Y. J., Remer, L. A., Tanré, D., Slutsker, I., and Holben, B. N.: A spatio-temporal approach for global validation and analysis of MODIS aerosol products, Geophysical Research Letters, 29, MOD1–1–MOD1–4, doi:10.1029/2001GL013206, http://dx.doi.org/10.1029/2001GL013206, 2002.

Justice, C., Giglio, L., Korontzi, S., Owens, J., Morisette, J., Roy, D., Descloitres, J., Alleaume, S., Petitcolin, F., and Kaufman, Y.: The {MODIS} fire products, Remote Sensing of Environment, 83, 244 – 262, doi:https://doi.org/10.1016/S0034-4257(02)00076-7, http://www.sciencedirect.com/science/article/pii/S0034425702000767, the Moderate Resolution Imaging Spectroradiometer (MODIS): a new generation of Land Surface Monitoring, 2002.

Justice, C. O., Giglio, L., Roy, D., Boschetti, L., Csiszar, I., Davies, D., Korontzi, S., Schroeder, W., O'Neal, K., and Morisette, J.: MODIS-Derived Global Fire Products, pp. 661–679, Springer New York, New York, NY, doi:10.1007/978-1-4419-6749-7_29, http://dx.doi.org/10.1007/978-1-4419-6749-7_29, 2011.

Kacenelenbogen, M., Vaughan, M. A., Redemann, J., Hoff, R. M., Rogers, R. R., Ferrare, R. A., Russell, P. B., Hostetler, C. A., Hair, J. W., and Holben, B. N.: An accuracy assessment of the CALIOP/CALIPSO version 2/version 3 daytime aerosol extinction product based on a detailed multi-sensor, multi-platform case study, Atmospheric Chemistry and Physics, 11, 3981–4000, doi:10.5194/acp-11-3981-2011, https://www.atmos-chem-phys.net/11/3981/2011/, 2011.

Kittaka, C., Winker, D. M., Vaughan, M. A., Omar, A., and Remer, L. A.: Intercomparison of column aerosol optical depths from CALIPSO and MODIS-Aqua, Atmospheric Measurement Techniques, 4, 131–141, doi:10.5194/amt-4-131-2011, http://www.atmos-meas-tech.net/4/131/2011/, 2011.

Konovalov, I. B., Beekmann, M., Kuznetsova, I. N., Yurova, A., and Zvyagintsev, A. M.: Atmospheric impacts of the 2010 Russian wildfires: integrating modelling and measurements of an extreme air pollution episode in the Moscow region, Atmospheric Chemistry and Physics, 11, 10 031–10 056, doi:10.5194/acp-11-10031-2011, http://www.atmos-chem-phys.net/11/10031/2011/, 2011.

Levy, R. C., Remer, L. A., and Dubovik, O.: Global aerosol optical properties and application to Moderate Resolution Imaging Spectroradiometer aerosol retrieval over land, Journal of Geophysical Research: Atmospheres, 112, n/a–n/a, doi:10.1029/2006JD007815, http://dx.doi.org/10.1029/2006JD007815, d13210, 2007.

Levy, R. C., Remer, L. A., Kleidman, R. G., Mattoo, S., Ichoku, C., Kahn, R., and Eck, T. F.: Global evaluation of the Collection 5 MODIS dark-target aerosol products over land, Atmospheric Chemistry and Physics, 10, 10 399–10 420, doi:10.5194/acp-10-10399-2010, http://www.atmos-chem-phys.net/10/10399/2010/, 2010.

Levy, R. C., Mattoo, S., Munchak, L. A., Remer, L. A., Sayer, A. M., Patadia, F., and Hsu, N. C.: The Collection 6 MODIS aerosol products over land and ocean, Atmospheric Measurement Techniques, 6, 2989–3034, doi:10.5194/amt-6-2989-2013, http://www.atmos-meas-tech.net/6/2989/2013/, 2013.

Ma, X., Bartlett, K., Harmon, K., and Yu, F.: Comparison of AOD between CALIPSO and MODIS: significant differences over major dust and biomass burning regions, Atmospheric Measurement Techniques, 6, 2391–2401, doi:10.5194/amt-6-2391-2013, http://www.atmos-meas-tech.net/6/2391/2013/, 2013.

Milinevsky, G., Danylevsky, V., Bovchaliuk, V., Bovchaliuk, A., Goloub, P., Dubovik, O., Kabashnikov, V., Chaikovsky, A., Miatselskaya, N., Mishchenko, M., and Sosonkin, M.: Aerosol seasonal variations over urbanâ€“industrial regions in Ukraine according to AERONET and POLDER measurements, Atmospheric Measurement Techniques, 7, 1459–1474, doi:10.5194/amt-7-1459-2014, http://www.atmos-meas-tech.net/7/1459/2014/, 2014.

Omar, A. H., Won, J.-G., Winker, D. M., Yoon, S.-C., Dubovik, O., and McCormick, M. P.: Development of global aerosol models using cluster analysis of Aerosol Robotic Network (AERONET) measurements, Journal of Geophysical Research: Atmospheres, 110, n/a–n/a, doi:10.1029/2004JD004874, http://dx.doi.org/10.1029/2004JD004874, d10S14, 2005.

Omar, A. H., Winker, D. M., Vaughan, M. A., Hu, Y., Trepte, C. R., Ferrare, R. A., Lee, K.-P., Hostetler, C. A., Kittaka, C., Rogers, R. R., Kuehn, R. E., and Liu, Z.: The CALIPSO Automated Aerosol Classification and Lidar Ratio Selection Algorithm, Journal of Atmospheric and Oceanic Technology, 26, 1994–2014, doi:10.1175/2009JTECHA1231.1, http://dx.doi.org/10.1175/2009JTECHA1231.1, 2009.

Omar, A. H., Winker, D. M., Tackett, J. L., Giles, D. M., Kar, J., Liu, Z., Vaughan, M. A., Powell, K. A., and Trepte, C. R.: CALIOP and AERONET aerosol optical depth comparisons: One size fits none, Journal of Geophysical Research: Atmospheres, 118, 4748–4766, doi:10.1002/jgrd.50330, http://dx.doi.org/10.1002/jgrd.50330, 2013.

O'Neill, N. T., Eck, T. F., Smirnov, A., Holben, B. N., and Thulasiraman, S.: Spectral discrimination of coarse and fine mode optical depth, Journal of Geophysical Research: Atmospheres, 108, n/a–n/a, doi:10.1029/2002JD002975, http://dx.doi.org/10.1029/2002JD002975, 4559, 2003.

Péré, J. C., Bessagnet, B., Mallet, M., Waquet, F., Chiapello, I., Minvielle, F., Pont, V., and Menut, L.: Direct radiative effect of the Russian wildfires and its impact on air temperature and atmospheric dynamics during August 2010, Atmospheric Chemistry and Physics, 14, 1999–2013, doi:10.5194/acp-14-1999-2014, http://www.atmos-chem-phys.net/14/1999/2014/, 2014.

Redemann, J., Vaughan, M. A., Zhang, Q., Shinozuka, Y., Russell, P. B., Livingston, J. M., Kacenelenbogen, M., and Remer, L. A.: The comparison of MODIS-Aqua (C5) and CALIOP (V2 V3) aerosol optical depth, Atmospheric Chemistry and Physics, 12, 3025–3043, doi:10.5194/acp-12-3025-2012, https://www.atmos-chem-phys.net/12/3025/2012/, 2012.

Remer, L. A., Kaufman, Y. J., Tanré, D., Mattoo, S., Chu, D. A., Martins, J. V., Li, R.-R., Ichoku, C., Levy, R. C., Kleidman, R. G., Eck, T. F., Vermote, E., and Holben, B. N.: The MODIS Aerosol Algorithm, Products, and Validation, Journal of the Atmospheric Sciences, 62, 947–973, doi:10.1175/JAS3385.1, http://dx.doi.org/10.1175/JAS3385.1, 2005.

Remer, L. A., Kleidman, R. G., Levy, R. C., Kaufman, Y. J., Tanré, D., Mattoo, S., Martins, J. V., Ichoku, C., Koren, I., Yu, H., and Holben, B. N.: Global aerosol climatology from the MODIS satellite sensors, Journal of Geophysical Research: Atmospheres, 113, n/a–n/a, doi:10.1029/2007JD009661, http://dx.doi.org/10.1029/2007JD009661, d14S07, 2008.

Schroeder, W., Prins, E., Giglio, L., Csiszar, I., Schmidt, C., Morisette, J., and Morton, D.: Validation of {GOES} and {MODIS} active fire detection products using {ASTER} and ETM+ data, Remote Sensing of Environment, 112, 2711 – 2726, doi:https://doi.org/10.1016/j.rse.2008.01.005, http://www.sciencedirect.com/science/article/pii/S0034425708000102, earth Observations for Terrestrial Biodiversity and Ecosystems Special Issue, 2008.

Seiler, W. and Crutzen, P. J.: Estimates of gross and net fluxes of carbon between the biosphere and the atmosphere from biomass burning, Climatic Change, 2, 207–247, doi:10.1007/BF00137988, https://doi.org/10.1007/BF00137988, 1980.

Smirnov, A., Holben, B., Eck, T., Dubovik, O., and Slutsker, I.: Cloud-Screening and Quality Control Algorithms for the {AERONET} Database, Remote Sensing of Environment, 73, 337 – 349, doi:https://doi.org/10.1016/S0034-4257(00)00109-7, http://www.sciencedirect.com/science/article/pii/S0034425700001097, 2000.

Stohl, A.: Chapter 21 Computation, accuracy and applications of trajectories— a review and bibliography, Developments in Environmental Science, 1, 615 – 654, doi:http://dx.doi.org/10.1016/S1474-8177(02)80024-9, http://www.sciencedirect.com/science/article/pii/S1474817702800249, 2002.

Vaughan, M. A., Powell, K. A., Winker, D. M., Hostetler, C. A., Kuehn, R. E., Hunt, W. H., Getzewich, B. J., Young, S. A., Liu, Z., and McGill, M. J.: Fully Automated Detection of Cloud and Aerosol Layers in the CALIPSO Lidar Measurements, Journal of Atmospheric and Oceanic Technology, 26, 2034–2050, doi:10.1175/2009JTECHA1228.1, http://dx.doi.org/10.1175/2009JTECHA1228.1, 2009.

Winker, D. M., Pelon, J. R., and McCormick, M. P.: The CALIPSO mission: spaceborne lidar for observation of aerosols and clouds, doi:10.1117/12.466539, http://dx.doi.org/10.1117/12.466539, 2003.

Winker, D. M., Vaughan, M. A., Omar, A., Hu, Y., Powell, K. A., Liu, Z., Hunt, W. H., and Young, S. A.: Overview of the CALIPSO Mission and CALIOP Data Processing Algorithms, Journal of Atmospheric and Oceanic Technology, 26, 2310–2323, doi:10.1175/2009JTECHA1281.1, http://dx.doi.org/10.1175/2009JTECHA1281.1, 2009.

Winker, D. M., Pelon, J., Jr., J. A. C., Ackerman, S. A., Charlson, R. J., Colarco, P. R., Flamant, P., Fu, Q., Hoff, R. M., Kittaka, C., Kubar, T. L., Treut, H. L., McCormick, M. P., Mégie, G., Poole, L., Powell, K., Trepte, C., Vaughan, M. A., and Wielicki, B. A.: The CALIPSO Mission: A Global 3D View of Aerosols and Clouds, Bulletin of the American Meteorological Society, 91, 1211–1229, doi:10.1175/2010BAMS3009.1, http://dx.doi.org/10.1175/2010BAMS3009.1, 2010.

Witte, J. C., Douglass, A. R., da Silva, A., Torres, O., Levy, R., and Duncan, B. N.: NASA A-Train and Terra observations of the 2010 Russian wildfires, Atmospheric Chemistry and Physics, 11, 9287–9301, doi:10.5194/acp-11-9287-2011, http://www.atmos-chem-phys.net/11/9287/2011/, 2011.

Young, S. A., Vaughan, M. A., Kuehn, R. E., and Winker, D. M.: The Retrieval of Profiles of Particulate Extinction from Cloud–Aerosol Lidar and Infrared Pathfinder Satellite Observations (CALIPSO) Data: Uncertainty and Error Sensitivity Analyses, Journal of Atmospheric and Oceanic Technology, 30, 395–428, doi:10.1175/JTECH-D-12-00046.1, http://dx.doi.org/10.1175/JTECH-D-12-00046.1, 2013.

Atmos. Meas. Tech. Discuss., https://doi.org/10.5194/amt-2017-336
Manuscript under review for journal Atmos. Meas. Tech.
Discussion started: 12 October 2017

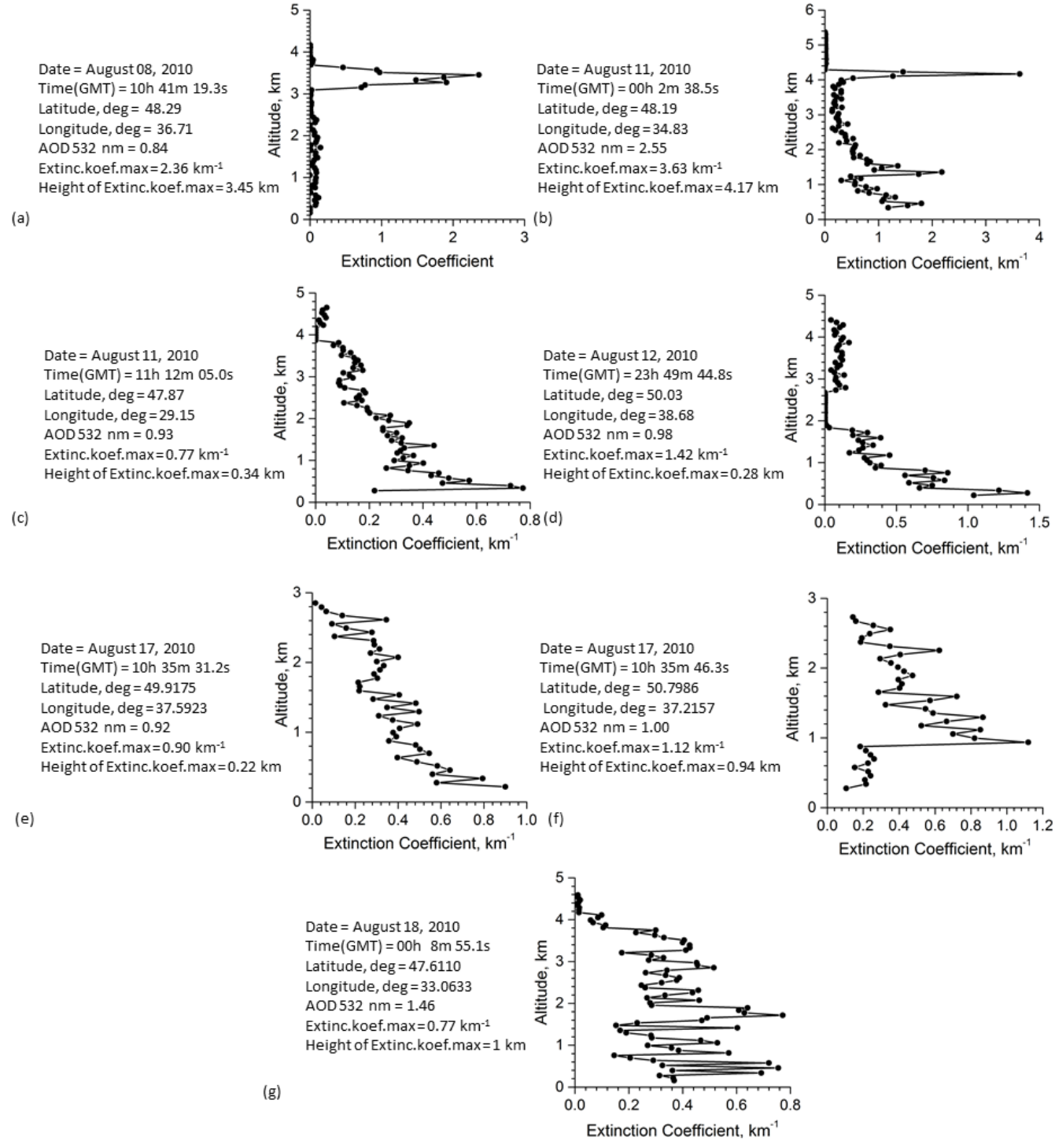

Figure 9. Typical vertical profiles of the aerosols extinction coefficient from CALIOP measurements over Ukraine during active fires period in summer 2010.